THE MICROWAVE SPECTRA OF TWO HALOGENATED PYRIMIDINES

CHRIS D. PAULSE

The Microwave Spectra of Two Halogenated Pyrimidines

Chris D. Paulse

Submitted in partial fulfillment of the requirements

for the degree of Master of Science

Chemistry Department

Memorial University of Newfoundland

St. John's, Nfld.

Canada, A1B 3X7

May 21, 1990

ISBN 0-315-68280-9

Acknowledgements

I would like to express gratitude to my supervisors Dr. R. W. Davis and Dr. R. A. Poirier for their useful advice and patient guidance over the last two years. I am grateful to Mr. R. Dodge for the generous allocation of computer resources which made many of the calculations presented here possible. I would also like to thank Mr. Junyi Chen and Dr. J. C. Lewis for interesting and stimulating discussions.

Abstract

The microwave spectra of seven isotopomers of 2-chloropyrimidine have been measured in the 33-80 GHz frequency range. These data have been analysed to yield, in the first instance, values of rotational constants, quartic centrifugal distortion constants and chlorine nuclear quadrupole coupling constants. The isotopic rotational constants confirm that the molecule is planar and has C_{2v} symmetry and have allowed the determination of partial substitution and ground state effective molecular geometries. For the normal isotopic species the pure rotational spectra of the molecule in five excited vibrational states have been observed and assignments made to vibrational quantum numbers on the bases of the observed inertial defects. A careful analysis of the nitrogen nuclear quadrupole hyperfine structure for the molecule 2-fluoropyrimidine is also presented. The experimental values of chlorine and nitrogen nuclear quadrupole coupling constants determined here are compared with the results of *ab initio* SCF calculations of the electric field gradients at the chlorine and nitrogen nuclei using a series of contracted Gaussian basis sets.

Contents

List of Tables

List of Figures

1 Introduction

The term microwave spectroscopy is synonymous with rotational spectroscopy, as the majority of molecules in the gas phase undergo rotational transitions by absorbing radiation in the microwave region of the spectrum. A high degree of resolution is obtainable in this region, which makes convenient the precise determination of energy levels in molecular rotational states. Rotational spectroscopy serves as a powerful tool in the determination of molecular structures, intra-molecular potential functions, and information about the electronic structure of the molecule through the measurement of dipole and quadrupole moments, and various hyperfine coupling constants.

The degree of resolution attainable from conventional microwave sources is typically of the order of kHz or better, with spectral features being measured to a halfwidth normally of 100 kHz or better under favourable experimental conditions. This kind of resolving power has been available for a number of years, and continues to be superior to that attainable in any other region of the spectrum, although recent developments using non-linear solid state devices have made possible the detailed study of the far infra red region using coherent radiation [1]. Furthermore, the advent of supersonic expansions have reduced observable experimental linewidths in many experiments to within the doppler limit [2].

This thesis reports and gives some interpretation of the microwave spectra of two closely related molecules, 2-fluoropyrimidine, and 2-chloropyrimidine. A short background to the theory of rotational energy levels is given as a summary. More detailed discussion of this theory can be found in a number of good textbooks [3, 4, 5]

1.1 Molecular Rotational Energy Levels

1.1.1 Angular Momentum

The coordinates of the nuclei of a freely rotating molecule can be represented in either the space fixed ($F = X, Y, Z$) or molecule fixed ($g = x, y, z$) axes. If we choose these coordinate systems to have the same origin, transformation may take place from one coordinate system to the other through a unitary matrix with elements given by the direction cosines

$$g = \sum_F \Phi_{Fg} F$$

$$F = \sum_g \Phi_{Fg} g$$

The corresponding angular momentum operators may also be formed in either basis, with the direction cosines again providing the transformation between them.

The angular momentum operators satisfy the standard commutation relations given in either coordinate system, with the convention that the anomalous sign be given to the commutators in the molecule fixed axis system. The square of the total angular momentum may be expressed either as

$$\mathbf{J}^2 = J_X^2 + J_Y^2 + J_Z^2$$

or

$$\mathbf{J}^2 = J_x^2 + J_y^2 + J_z^2$$

also

$$\mathbf{J}^2 J_F - J_F \mathbf{J}^2 = 0$$

and

$$\mathbf{J}^2 J_g - J_g \mathbf{J}^2 = 0$$

We choose a set of eigenfunctions which simultaneously diagonalizes **J** and J_Z or **J** and J_z with diagonal matrix elements given by

$$\langle J,K,M|J^2|J,K,M\rangle = J(J+1)$$

$$\langle J,K,M|J_Z|J,K,M\rangle = M$$

$$\langle J,K,M|J_z|J,K,M\rangle = K$$

It is convenient to construct ladder operators defined as

$$J_{F\pm} = J_X \pm iJ_Y$$

$$J_{g\pm} = J_x \pm iJ_y$$

which leads to non vanishing off diagonal matrix elements given by

$$\langle J,K-1|J_{g\pm}|J,K\rangle = [J(J+1) - K(K+1)]^{\frac{1}{2}}$$

1.1.2 Kinetic Energy of a Rotating Rigid Body

To a good approximation, the angular momentum of a rotating molecule may be described by a set of point masses with fixed internal coordinates. The kinetic energy of the molecule may be expressed as

$$T_R = I_{xx}\omega_x^2 + I_{yy}\omega_y^2 + I_{zz}\omega_z^2$$

where $\omega_{gg}(g = x,y,z)$ are the components of the angular velocity in the x,y, and z directions, and the moments of inertia are defined in the principal axes as

$$I_{xx} = \sum m_i(y_i^2 + z_i^2)$$

$$I_{yy} = \sum m_i(z_i^2 + x_i^2)$$

$$I_{zz} = \sum m_i(x_i^2 + y_i^2)$$

with

$$\sum m_i x_i y_i = \sum m_i y_i z_i = \sum m_i x_i z_i = 0$$

For symmetric tops, two of the moments of inertia are equal (i.e. $I_{xx} = I_{yy} \neq I_{zz}$) and the z axis is usually referred to as the symmetry axis. The angular velocity may be replaced by the angular momentum, and we define the rotational constants as

$$B = \frac{h}{8\pi^2 I_{xx}}$$

$$A \text{ or } C = \frac{h}{8\pi^2 I_{zz}}$$

with the convention that $A \geq B \geq C$. When $I_{xx} > I_{zz}$ A should be used above, and the molecule is classified as a prolate symmetric top. When $I_{xx} < I_{zz}$, C should be used, and the molecule is then described as an oblate symmetric top. With the commutation relations established in the previous section, we may now construct a Hamiltonian for either case as

$$\mathbf{H_R}/h = B\mathbf{J}^2 + (A - C)J_z^2$$

for a prolate rotor, and

$$\mathbf{H_R}/h = B\mathbf{J}^2 + (C - B)J_z^2$$

for an oblate rotor. $\mathbf{H_R}$ can be shown to commute with $\mathbf{J}^2$, J_z, and J_Z, so we choose the same basis $|J, K, M\rangle$ as given before, and find the matrix elements given by

$$\langle J, K, M|H_R/h|J', K', M'\rangle = (E_R/h)\delta_{JJ'}\delta_{KK'}\delta_{MM'}$$

where $\delta_{JJ'}$, $\delta_{KK'}$, and $\delta_{MM'}$ represent the Dirac delta function. with the energy levels of a rigid symmetric top given by

$$E_R = BJ(J+1) + (A-B)K^2 \qquad \text{(prolate)}$$

$$E_R = BJ(J+1) + (C-B)K^2 \qquad \text{(oblate)}$$

where J is the principal angular momentum quantum number, and K represents the magnitude of rotation about the symmetry axis. Rotational energy levels described by J and K are doubly degenerate. It is convenient to introduce the Wang symmetric rotor functions at this point, defined by

$$S(J,K,M,\gamma) = \frac{1}{\sqrt{2}}[|J,K,M\rangle + (-1)^{\gamma}|J,-K,M\rangle]$$

where γ represents the *parity* of the rotational wavefunction and can take values of either 0 or 1. and note that the eigenfunctions in the symmetric rotor basis may be obtained by successive applications of the defined ladder operators to the spherical harmonic of a linear molecule:

$$|J,\pm|K|,\pm|M|\rangle = N J_{g\pm}^{|K|} J_{F\pm}^{|M|} |J,0,0\rangle$$

where N is a normalization factor.

The Hamiltonian for the asymmetric top is given as

$$\mathbf{H_R}/h = AJ_a^2 + BJ_b^2 + CJ_c^2$$

with x,y, and z here replaced by a,b, and c. The Hamiltonian is invariant to the symmetry operations E, C_2^a, C_2^b, and C_2^c and belongs to the four group (V). The K degeneracy observed in symmetric tops is now removed, and this quantum number is replaced by two 'pseudo'

quantum numbers normally designated as K_A and K_C, representing the value K would take in the limiting cases of the oblate and prolate top. It is convenient to introduce Ray's asymmetry parameter κ defined as

$$\kappa = \frac{2B - A - C}{A - C}$$

as a measure of asymmetry which takes limiting values of -1 for a prolate top and +1 for an oblate top. Rotational levels as a function of the asymmetry are visualised with the aid of an energy level diagram in Figure 1.1 for the $J = 2$ rotational state. The removal of this degeneracy gives rise to "asymmetry splitting" in microwave spectra, and for severely asymmetric molecules, leads to complex spectral patterns. Expressions for the asymmetric rotor wavefunctions are formed from linear combinations of symmetric rotor functions

$$\psi_{J K_A K_C} = \sum_{J,K,M} a_{JKM} \psi_{JKM}$$

and may also be expressed in terms of the Wang functions given above as

$$\psi_{J K_A K_C} = \sum_{J,K,M} a_{JKM} S(J, K, M, \gamma)$$

It is convenient to continue using the Wang functions as the basis for the asymmetric rotor functions, as they may be factored according to the symmetry of the wave function. The four group gives rise to four distinct symmetry species A,B_a,B_b, and B_c and the asymmetric rotor wave function must belong to one of these species. The symmetry of the asymmetric rotor function is conveniently given by the evenness of oddness of the two K subscripts, and we may classify the functions as given in Table 1.1.

With the symmetry classification of rotational energy levels, the energy matrix may be factored into four distinct sub-matrices, given the names $\mathbf{E}^+$, $\mathbf{E}^-$, $\mathbf{O}^+$, and $\mathbf{O}^-$. These

Table 1.1: Parity of Asymmetric Rotor Eigenfunctions

V	E	C_2^a	C_2^b	C_2^c	K_A	K_C
A	1	1	1	1	e	e
B_a	1	1	-1	-1	e	o
B_b	1	-1	1	-1	o	o
B_c	1	-1	-1	1	o	e

matrices are no longer diagonal, and thus explicit expressions for rotational energies are no longer available, except for $J \leq 3$. Solutions are normally obtained through numerical diagonalization techniques on a digital computer.

1.2 Molecular Structure Determination

One of the goals of microwave spectroscopists is the determination of state specific molecular geometries. Perhaps the most easily calculated spectroscopic geometry is the ground state structure, denoted as r_0. This structure is obtained usually for small molecules from a small set of ground state rotational constants. Structures obtained in this way are often unreliable due to the fact that zero point vibrational effects remain unaccounted for, which especially for bonds involving hydrogen, may lead to unrealistic values and may not be directly compared with geometries obtained from theoretical calculations.

An alternative structure may be obtained from isotopic substitution in a molecule and is called the *substitution structure.* From the microwave spectra of a number of isotopomers of

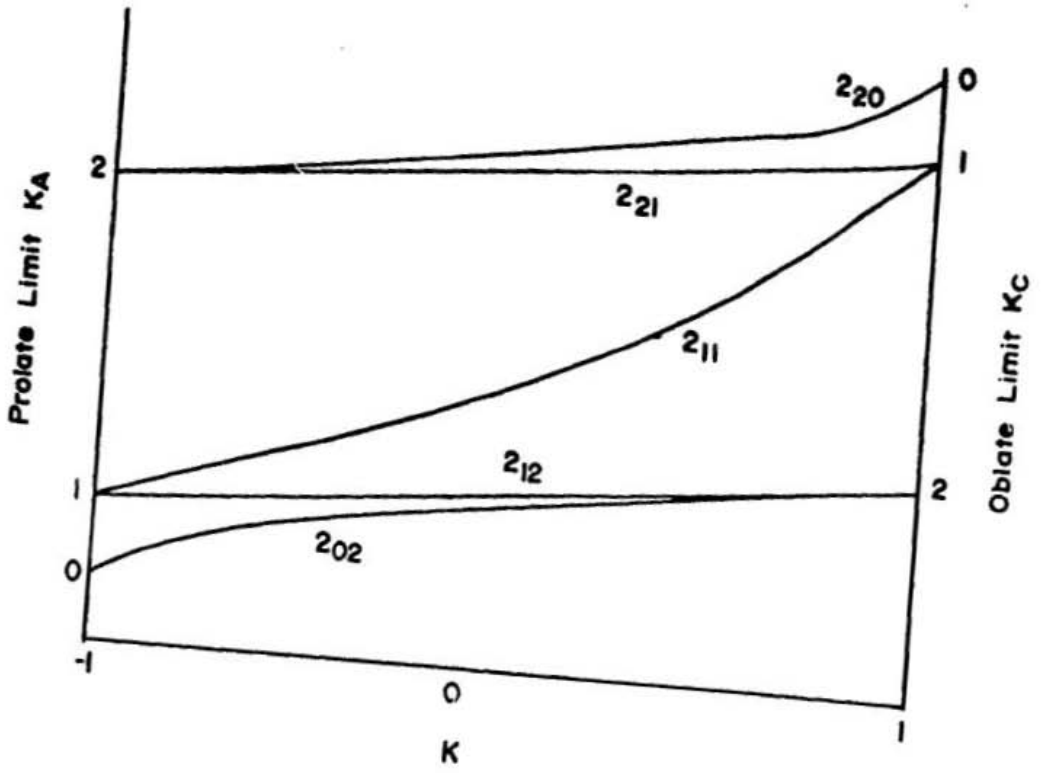

Figure I.1 Energy Levels of an Asymmetric Top with J=2 as a Function of Asymmetry K Calculated for A=5 and C=3.

the molecule of interest, substitution coordinates of the nuclei are obtained from differences in their ground state moments of inertia (Kraitchman's equations [6]). Structures obtained in this way are generally reliable approximations of the equilibrium geometry, however if a nucleus lies close to one of the inertial axes, its substitution coordinate may be largely in error. This problem can in some cases be ameliorated by employing the method known as double substitution [7].

Accordingly, the coordinate is obtained from second differences in the moments of inertia with the substitution of two nuclei, giving rise to three distinct sets of rotational constants. For symmetric substitution along a symmetry axis:

$$\Delta I_{jk} - \Delta I_j = (\mu_j^{'} - \mu_j) - 2(\mu_j^{'}\Delta r_k)r_j + \mu_j^{'}(\Delta r_k)^2$$

where

$$\Delta r_k = \frac{\Delta m_k r_k}{M + \Delta m_k}$$

$$\mu_j = \frac{M\Delta m_j}{M + \Delta m_j}$$

$$\Delta I_{jk} = I_{jk} - I_k$$

r_j and r_k are the substitution coordinates of nuclei j and k, M is the parent mass, and Δm is the change in mass with isotopic substitution. The solution of this quadratic equation gives the substitution coordinate r_j of the nucleus.

1.3 Nuclear Quadrupole Coupling

In rotational spectra angular momentum coupling between the nuclear moments and the molecular field may be due to either electric or magnetic interactions. Nuclear electric

coupling is the most important of these phenomena for closed shell molecules and is given rise to by interaction of a nuclear electric quadrupole with the molecular electric field gradient. Magnetic hyperfine structure in rotational spectra is caused by interaction of the nuclear magnetic dipole with the molecular magnetic field. This effect is considerably smaller in typical spectra and is not considered here. The interested reader is instead referred to reviews of the subject [5].

In order for a nucleus to exhibit quadrupole coupling, it must have a quadrupole moment, or non spherical distribution of electric charge. Nuclei with spins of 0 or $\frac{1}{2}$ are spherically symmetric, posses no quadrupole moment and do not give rise to electric hyperfine structure. Experimental information of this type is informative in the probing of molecular electronic structures, and approximate molecular electronic wave functions may be used to predict observable hyperfine patterns from calculated electric field gradients [8].

The effect of the nuclear quadrupole interaction in a rotating molecule is to couple the nuclear spin **I**, with the molecular rotational angular momentum **J** to form a resultant overall angular momentum **F**. This coupling can be shown with the help of a vector diagram (Figure 1.2) to be a precession of **I** and **J** around **F**. The Hamiltonian for this interaction is given as

$$\mathbf{H}_Q = -\frac{1}{6}\mathbf{Q} \cdot \nabla \mathbf{E}$$

Both the electric field gradient and the nuclear quadrupole tensor are symmetric and traceless in Cartesian coordinates and may be represented by irreducible spherical tensors of rank two.

$$\mathcal{H}_Q = \mathbf{V}^{(2)} \cdot \mathbf{Q}^{(2)}$$

We choose as our basis for the asymmetric top $|J\tau IFM_F)$ where J has its usual meaning, $\tau = K_A - K_C$, I is the nuclear spin quantum number, F is the overall angular momentum

quantum number and M_F gives the projection of F along the axis of quantization. The matrix elements of this scalar product can be generated in terms of the six-j symbol and the reduced matrix elements as

$$(\tau' J' I F|\mathbf{V^{(2)}}\cdot\mathbf{Q^{(2)}}|\tau J I F) = (-1)^{J+I+F}\left\{\begin{array}{ccc} F & I & J' \\ 2 & J & I \end{array}\right\}(\tau' J'||V^{(2)}||\tau J)(I||Q||I)$$

The reduced matrix elements elements above may be given in terms of the nuclear quadrupole moment and the electric field gradient using the Wigner 3-j symbols with I and J taking maximum projection along the z axis as

$$\frac{1}{2}(eQ) = (II|Q_0^{(2)}|II) = \left(\begin{array}{ccc} I & 2 & I \\ -I & 0 & I \end{array}\right)(I||Q^{(2)}||I)$$

and

$$(\tau' J' J'|V_0^{(2)}|\tau J J) = (-1)^{J'-J}\left(\begin{array}{ccc} J' & 2 & J \\ -J & 0 & J \end{array}\right)(\tau' J'||V^{(2)}||\tau J)$$

The 3-j symbol takes explicit values in the cases given above for the non zero matrix elements [9]. If we treat the single nucleus coupling problem using first order perturbation, all elements off diagonal in J disappear, and J becomes a good quantum number. Quadrupolar energy expressions may be fashioned explicitly at this level in terms of the direction cosine matrix elements

$$eQq_J = \langle\chi_{zz}\rangle = \langle\Phi_{Za}^2\rangle\chi_{aa} + \langle\Phi_{Zb}^2\rangle\chi_{bb} + \langle\Phi_{Zc}^2\rangle\chi_{cc}$$

or the angular momentum expectation values

$$eQq_J = \frac{2}{(J+1)(2J+3)}\sum_g\langle J_g^2\rangle\chi_{gg}$$

with the total expression for E_Q now given by

$$E_Q = [\frac{eQq_J(2J+3)}{J}]Y(I,J,F)$$

where the expression involving the six-j and 3-j symbols has now been reduced and is given by the well known Casimir's function

$$Y(I,J,F) = \frac{\frac{3}{4}C(C+1) - I(I+1)J(J+1)}{2(2J+3)(2J-1)(2I-1)}$$

where

$$C = F(F+1) - I(I+1) - J(J+1)$$

With the values of $\langle J_a^2 \rangle$ obtained from the eigenvectors of the asymmetric rotor rotational Hamiltonian and the Wang reduced energy $W(b)$ [3], the diagonal matrix elements, and hence the quadrupolar energy terms may be conveniently expressed in terms of the tensor element along the principal inertial axis χ_{aa} and the asymmetry η as

$$E_Q = \frac{\chi_{aa}}{(J+1)(2J+3)}\{3\langle J_a^2\rangle - J(J+1) + [\langle J_a^2\rangle - W(b_p)]\frac{\eta}{b_p}\}Y(I,J,F)$$

for a near prolate asymmetric top and

$$E_Q = \frac{\chi_{aa}}{(J+1)(2J+3)}\{3\langle J_c^2\rangle - J(J+1) + [\langle J_c^2\rangle - W(b_o)]\frac{\eta}{b_o}\}Y(I,J,F)$$

for a near oblate asymmetric top, where

$$\eta = \frac{\chi_{bb} - \chi_{cc}}{\chi_{aa}}$$

$$b_p = \frac{C-B}{2A-B-C}$$

and

$$b_o = \frac{A-B}{2C-B-A}$$

In assigning F quantum numbers to the hyperfine features, use was made of the formulae for relative intensities of hyperfine components [3]. The quadrupole coupling constants are

obtained from the observed splittings of the rotational lines by assigning values of F to the hyperfine components using the scheme

$$\nu_2 - \nu_1 = E_Q(F_2', J_2') - E_Q(F_2, J_2) - E_Q(F_1', J_1') + E_Q(F_1, J_1)$$

and linear least squares. The matrix relation for deriving least squares quantities is given as

$$\mathbf{A}x = y$$

where y is a vector containing the data, $\mathbf{A}$ is an m x n matrix constructed from our chosen basis functions, and x is the solution vector containing the quadrupole coupling constants, here given as χ_{aa} and $(\chi_{bb} - \chi_{cc})$. For higher J transitions, coalescence of pairs of hyperfine components is normally observed, and it is therefore necessary to use data weighting. The method of Singular Value Decomposition [14] was used to solve the overdetermined linear system given above and error estimates on the derived parameters were obtained using standard techniques.

Two angular momentum coupling schemes arise for the case of interaction by two quadrupolar nuclei. In the case where the coupling is nearly equivalent, the scheme of $I_1 + I_2 = I$ and $I + J = F$ is most conveniently employed whereas for the case where the coupling of one nucleus exceeds in magnitude that of the other, the scheme $I_1 + J = F_1$ and $F_1 + I_2 = F$ is best used. The general form of the Hamiltonian for this system is

$$\mathcal{H} = \mathcal{H}(1) + \mathcal{H}(2)$$

or

$$\mathcal{H} = \frac{1}{6}[\mathbf{Q}(1) \cdot \nabla\mathbf{E}(1) + \mathbf{Q}(2) \cdot \nabla\mathbf{E}(2)]$$

Considering first the case of plural nearly equal coupling, our basis is formed from $|J\tau I_1 I_2 I F M_F)$ and the matrix elements are given as

$$(\tau' J' I_1 I_2 I' F|\mathbf{Q}(1)\cdot\nabla\mathbf{E}(1)|\tau J I_1 I_2 I F) =$$

$$(-1)^t(eQq_{J'J})_1 f(J')f(I_1)[(2I+1)(2I'+1)]^{\frac{1}{2}} \begin{Bmatrix} F & I' & J' \\ 2 & J & I \end{Bmatrix} \begin{Bmatrix} I_1 & I' & I_2 \\ I & I_1 & 2 \end{Bmatrix}$$

with $t = J + I_1 + I_2 + I' + I + F$ and

$$(\tau' J' I_1 I_2 I' F|\mathbf{Q}(2)\cdot\nabla\mathbf{E}(2)|\tau J I_1 I_2 I F) =$$

$$(-1)^t(eQq_{J'J})_1 f(J')f(I_1)[(2I+1)(2I'+1)]^{\frac{1}{2}} \begin{Bmatrix} F & I' & J' \\ 2 & J & I \end{Bmatrix} \begin{Bmatrix} I_1 & I' & I_2 \\ I & I_1 & 2 \end{Bmatrix}$$

For plural coupling I is no longer a good quantum number and explicit expressions for the quadrupolar energy are no longer available except for special cases.

When the coupling from each nucleus is equivalent ($I_1 = I_2$) $(eQq_{J'J})_1 = (eQq_{J'J})_2$ and the matrix elements of the type $(I|I+1)$ disappear while matrix elements of the type $(I|I)$ and $(I|I+2)$ are nonvanishing, and for a given F, the energy matrix now factors into two submatrices for even and odd I. Formulas for the matrix elements required in this case have been given by Robinson and Cornwell [11] and Flygare and Gwinn [11]. Explicit expressions for the energy levels are also given in reference [11] for the case where $I_1 = I_2 = \frac{3}{2}$, from which it was possible to write linear least squares routines for the estimation of quadrupole coupling constants arising from the presence of two equivalent chlorine or nitrogen nuclei [12].

Hyperfine patterns arising from two nuclear couplings are generally more complex than those observed when only one quadrupolar nucleus is present and thus the coupling constants

were fit to deviations of the component from the unperturbed rotational line rather than the observed splittings between lines. Nuclear spin statistical weights play an important role in describing the relative intensities of the transitions and thus the assignment of I and F quantum numbers to the transitions required more effort than in the simpler case of a single coupling.

The case of two couplings arising from equivalent nitrogen nuclei will be discussed in detail. Nitrogen 14 has nuclear spin of 1 and in this case $I_1 = I_2 = 1$; thus I may take values of 0, 1, or 2. With our chosen basis of $|I_1 I_2 I J F M_F)$, the quadrupole Hamiltonian gives rise to five submatrices: one of dimension three for the case where $F = J$, two of dimension two where $F = J \pm 1$, and two of dimension one for the case where $F = J \pm 2$. The formulae for quadrupolar energy levels in this case have been derived by Dobyns and Pierce [13] in terms of χ_{zz}, the coupling along the principal axis of the bond and are given in Table 1.2. In labelling these energy levels, i is not a good quantum number, as the matrices generated by the Hamiltonian are not diagonal in i; but it serves the purpose of identifying a particular state.

As in the case of single coupling, χ_{zz} could be again expressed in terms of χ_{aa} and $(\chi_{bb} - \chi_{cc})$. For rotational transitions with $J > 10$ the hyperfine components of a prolate rotor with two equivalent nitrogen atoms coalesce into observable triplets. In this high J limit, the selection rule $\Delta I = \Delta J$ holds roughly, and the relative intensities of each hyperfine transition are given by the nuclear spin statistical weights of the lower state. It is possible from these intensities to accurately calculate the unperturbed rotational frequency of the triplet using the center of gravity [15]. From the unperturbed frequency calculated in this way, the splitting due to each hyperfine component could be determined to within the measurement

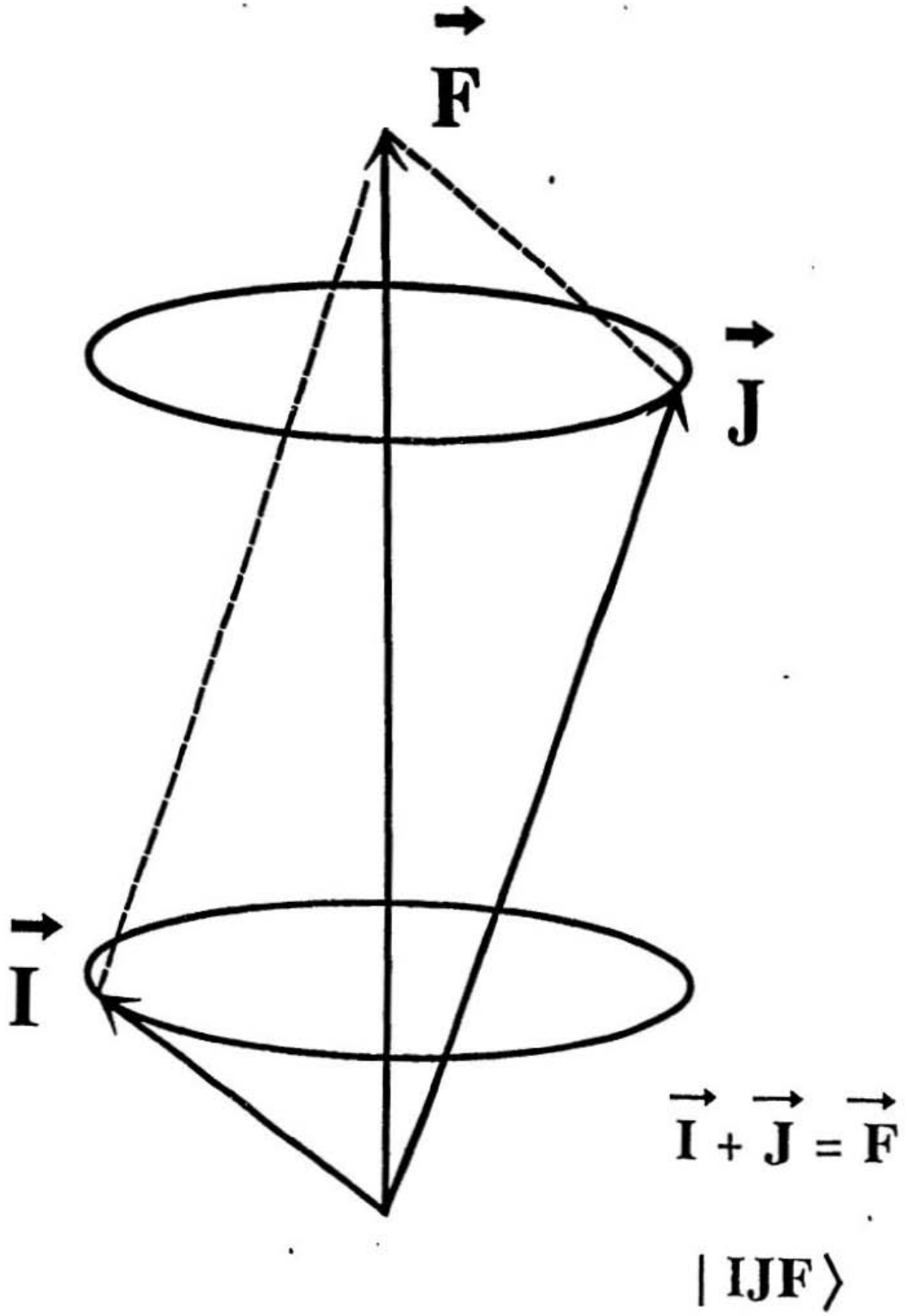

Figure 1.2: A Vector Diagram of the Coupling Between the Nuclear Spin Angular Momentum (I) and the Molecular Rotational Angular Momentum (J).

Table 1.2: Quadrupolar Energy Levels for Two Equal Couplings by Nuclei of Spin 1

F	i	$\lambda(i, J, F)$
$J+2$	2	$\frac{1}{2}$
$J+1$	2	$-\frac{J+6}{4J}$
J	2	$-\frac{(2J-3)(2J+5)-3\sqrt{16J^4+32J^3-8J^2-24J+25}}{8J(2J-1)}$
$J-1$	2	$-\frac{(2J+3)(J-5)}{4J(2J-1)}$
$J-2$	2	$\frac{(2J+3)(J+1)}{2J(2J-1)}$
$J+1$	1	$-\frac{1}{4}$
J	1	$\frac{2J+3}{4J}$
$J-1$	1	$-\frac{(J+1)(2J+3)}{2J(2J-1)}$
J	0	$-\frac{(2J-3)(2J+5)+3\sqrt{16J^4+32J^3-8J^2-24J+25}}{8J(2J-1)}$

accuracy of the spectrometer; using this data, the introduction of correlation of measurement error is avoided. Assignment of these splittings was made by transferring coupling constants that had been previously determined for a similar molecule, and predicting the patterns that should evolve. With a complete assignment of the components, the splittings are used in a least squares refinement. As stated by Dobyns and Pierce [13], the observed splittings in the Q branch transitions for an asymmetric top will be sufficient to determine the asymmetry of the quadrupole tensor. Splittings in R branch transitions are required to determine the principal element of the tensor.

1.4 Ab Initio Calculation of Electric Field Gradients

With values of the nuclear quadrupole moment, estimates of the electric field gradients at the nucleus obtained from *ab initio* or semi empirical calculations may be used to predict quadrupole coupling constants. The electric field gradient is a second rank tensor with components given as

$$q_A^{\alpha\beta} = \sum_{\mu\nu} P_{\mu\nu} \langle \phi_\mu | (r_A^2 \delta_{\alpha\beta} - 3 r_{A\alpha} r_{A\beta}) / r_A^5 | \phi_\nu \rangle + \sum_{B \neq A} Z_B (3 R_{AB\alpha} R_{AB\beta} - \delta_{\alpha\beta} R_{AB}^2) / R_{AB}^5$$

where $\alpha, \beta = x, y, z$; $P_{\mu\nu}$ is the one particle density matrix; ϕ_μ and ϕ_ν are atomic orbitals; R_{AB} is the internuclear distance; and r_A is the distance of the electron from nucleus A, $r_{A\alpha}$ is the cartesian coordinate distance of the electron from nucleus A, and $R_{AB\alpha}$ is the cartesian coordinate internuclear distance. The first term above represents the electronic contribution to the electric field gradient, while the second term represents the nuclear contribution.

For the calculations reported here, the reduced one particle density matrix was calculated from SCF molecular orbital coefficients with the atomic orbitals generated from standard

basis sets using the Gaussian 86 program suite [16].

References

[1] R. J. Saykally, Acc. Chem. Res. *in press* (1989).

[2] T. J. Balle, W. H. Flygare, Rev. Sci. Instrum. 52, 33 (1981).

[3] W. Gordy and R. L. Cook, Microwave Molecular Spectra, John Wiley, New York, 1984.

[4] H. Kroto, Molecular Rotational Spectra, Wiley-Interscience, New York,1975.

[5] Eizi Hirota, High Resolution Spectroscopy of Transient Molecules, Springer Series in Chemical Physics 40, Springer-Verlag, Berlin Heidelberg, 1985.

[6] J. Kraitchman, Am. J. Phys. 21, 17 (1953).

[7] L. Pierce, J. Mol. Spec. 3, 575 (1959).

[8] G. E. Scuseria, T. J. Lee, R. J. Saykally, and H. F. Schaefer, J. Chem. Phys. 84, 3711 (1986).

[9] A. R. Edmonds, Angular Momentum in Quantum Mechanics, Princeton Univ. Press, Princeton, 1960.

[10] G. H. Golub and C. Reinsch, Numer. Math. 14, 403 (1970).

[11] G. W. Robinson and C. D. Cornwell, J. Chem. Phys. 21, 1436 (1953).

[12] W. H. Flygare and W. D. Gwinn, J. Chem. Phys. 36, 787 (1962).

[13] The programs used in this work, including those for the calculation of single and plural equivalent couplings are available from the Quantum Chemistry Program Exchange at the University of Indiana.

[14] V. Dobyns and L. Pierce, J. Am. Chem. Soc. 85, 3553 (1963).

[15] H. Rudolph, Z. Naturforsch. 23a, 540 (1968).

[16] Gaussian 86, M. J. Frisch, J. S. Binkley, H. B. Schlegel, K. Raghavachari, C. F. Melius, R. L. Martin, J. J. P. Stewart, F. W. Bobrowicz, C. M. Rohlfing, L. R. Kahn, D. J. Defrees, R. Seeger, R. A. Whiteside, D. J. Fox, E. M. Fleuder, and John A. Pople, Carnegie-Mellon Quantum Chemistry Publishing Unit, Pittsburgh PA, 1984.

2 Experimental

2.1 Microwave Spectrometer

The microwave spectrometer used for the experiments described in this work is of conventional design employing Stark modulation [1]. The individual components making up the spectrometer are described in detail in the subsections given below.

2.1.1 Microwave Frequency Source

A Hewlett Packard model 8341A synthesized sweeper was used as a coherent source of continuous wave microwave frequency radiation. Microwaves are generated from a solid state electronically tuned oscillator, with tuning of the signal accomplished within the sweeper through the use of phase locking. Output signals from the sweeper were of high spectral purity with a bandwidth of less than 4 Hz. A number of passive radiofrequency multipliers were used to obtain frequency coverage from 8 to 80 GHz. Spectral purity within the waveguide was somewhat less than that produced from the synthesizer, and is estimated to be 1 kHz.

2.1.2 Waveguide

Samples were contained at low pressure inside a 10 foot long brass S-band waveguide. The cell was pumped with a Varian model SD-200 rotary vacuum pump backed with liquid nitrogen traps, which achieved pressures lower than 20 mtorr during the course of measurements. The Stark electrode was secured along the length of the waveguide with insulation from the outside of the cell provided by teflon mounts. Samples were introduced at one end of the

cell through a glass/metal o-ring adaptor, with a round bottomed flask used as a sample reservoir. The reservoir was cooled either using an ice/salt water bath, or in the case of volatile samples, a bath of dry ice.

2.1.3 Microwave Detection and Stark Modulation

Intervals of between 1 and 10 MHz were chosen as sweep widths for the measurement of rotational transitions. Frequency variation over these intervals was performed either directly by the sweeper, or through external control by a microcomputer. Stark modulation was applied with the use of a square wave generator operating at 33 kHz. Signals from the crystal detector were passed to a digital lock-in amplifier (EG&G Model 5207) locked to the frequency of the applied square wave potential in the cell. Microwave absorptions due to molecules perturbed by the applied electric field registered negative voltages on the lock-in, while zero field lines registered positive voltages. Accurate measurement of line centers was made by digitally sweeping the microwave signal over the frequency range of the absorption, and collecting a number of points at each frequency interval using a 12-bit A/D converter. These points were averaged to increase the signal to noise ratio thus giving an absorption peak with a characteristic Lorentzian lineshape. The points collected in this manner were fit to a simple Lorentzian function using the Marquardt algorithm [2]. From the parameters given by this refinement, it was possible to obtain the line center.

2.2 Preparation of Labelled Chloropyrimidines

Samples of ^{13}C and ^{15}N 2-chloropyrimidine were synthesized using isotopically enriched samples of ^{13}C and ^{15}N urea (MSD Isotopes) as starting materials. In the first step of the syn-

thesis, 1,3,3-tetraethoxypropane (5.5g) was added to a solution of the urea samples (1.5g) in ethanol (10 mL) and concentrated HCl (5 mL). The mixture was stirred for one hour and cooled with ice to yield solid 2-hydroxypyrimidine hydrochloride. The product was dissolved in aqueous sodium carbonate and acidified to pH 5 with sulfuric acid. The solution was evaporated to dryness and extracted with ethyl acetate (1.5 L). The extract yielded 2-hydroxypyrimidine [3].

Samples of 2-hydroxypyrimidine were added to a solution of PCl_5 in $OPCl_3$ (4 mL) and heated to 140°C for 45 minutes. The solution was made alkaline with NaOH and the chlorinated product was extracted with diethyl ether. Recrystalizations with petroleum ether yielded pure samples of 2-chloropyrimidine [4].

References

[1] S. Firth and R. W. Davis, J. Mol. Spectrosc. 127, 209 (1988).

[2] D. W. Marquardt, J. Soc. ind. appl. Math. 11, 431 (1961).

[3] R. R. Hunt, J. E. W. McOmie and E. R. Sayer, J. Chem. Soc. London 1959, 529 (1959).

[4] T. Matsukawa and B. Ohta, J. Pharm. Soc. Japan 69, 489 (1949).

3 Results

3.1 2-Chloropyrimidine

3.1.1 Microwave Spectra

Assignment of the microwave spectrum of 2-chloropyrimidine was started by obtaining guessed rotational constants from a hybrid molecular geometry obtained from the previously determined gas phase structures of pyrimidine [1] and chlorobenzene [2]. Although the spectrum was not accurately predicted in this way, clumps of high K_A a type R branches were quickly located and assigned. The assignment was then gradually extended to include the more widely scattered low K_A lines.

Once a complete assignment of the normal species was made, it was possible to fit the transitions to Watson's S-reduced Hamiltonian [3] in the I^r representation. Lines with large values of K_A showed significant splitting due to the presence of the quadrupolar chlorine nucleus, and unperturbed rotational frequencies were simply obtained from the center of gravity of the observed hyperfine doublet or quartet [4]. The measured rotational transitions of the normal species in its ground vibrational state are given in Table 3.1, with the corresponding rotational and determinable quartic centrifugal distortion constants given in Table 3.2. With an assignment of the normal species it was possible to search for the naturally occurring ^{37}Cl isotopomer. Searches were made for R branch transitions in the same way as was done for the normal species. From the lines measured for this species (Table 3.3), it was again possible to obtain accurate values of rotational constants, and quartic centrifugal distortion constants (Table 3.2).

The prepared isotopically labelled species of 2-chloropyrimidine were used without further purification. Searches for lines for these species were made with initial guesses of rotational constants from the normal species together with estimated changes due to isotopic substitution. The same strategy as outlined above was used in assigning these spectra. The measured rotational transitions of the prepared ^{13}C and ^{15}N labeled isotopomers of 2-chloropyrimidine are given in Tables 3.4-3.7 with their rotational and determinable quartic distortion constants given in Table 3.2.

It was possible to assign the spectrum of five vibrational sattelites of 2-chloropyrimidine (Tables 3.8-3.12), from which it was possible to obtain accurate values of rotational and some quartic centrifugal distortion constants (Table 3.13). The most highly populated vibrational state may be assigned to the out of plane bending mode of the C–Cl bond as indicated by its large negative inertial defect (-0.615) and the state measured to have $\Delta = -1.237$ was easily assigned as the v=2 level of this mode. The measured state with a large positive inertial defect is assigned to the B_2 type in-plane bend of the C–Cl bond. Two of the sattelites remain unassigned, but may be attributed to excited states of the four possible ring deformation modes.

Once an assignment of the spectra of the five most populated vibrational states of the normal species of 2-chloropyrimidine had been made, the most abundant naturally occurring ^{13}C species was searched for. The intensities of the transitions for this species were expected to be 2% of that observed for the normal species. Due to the low intensity of these lines, large numbers of scans were required in order to obtain reasonably well defined lineshapes. A total of 30 transitions were measured for this isotopomer (Table 3.14) from which accurate values of all three rotational constants could be obtained (Table 3.2).

Table 3.1: Rotational Transitions of 2-Chloropyrimidine

J_U	K_A	K_C		J_L	K_A	K_C	Obs / MHz	Obs-Calc	Weight
12	2	10	←	11	2	9	38411.346	0.019	1.000
12	0	12	←	11	0	11	33360.729	-0.034	1.000
13	11	3	←	12	11	2	39608.066	0.006	1.000
13	2	12	←	12	2	11	38277.668	0.020	1.000
13	1	12	←	12	1	11	39094.503	0.158	0.000
14	2	12	←	13	2	11	44455.980	-0.046	1.000
14	1	14	←	13	1	13	38612.601	-0.004	1.000
14	2	13	←	13	2	12	41043.279	-0.022	1.000
14	1	13	←	13	1	12	41692.269	0.021	1.000
15	2	13	←	14	2	12	47337.527	0.024	1.000
15	0	15	←	14	0	14	41310.945	0.00?	1.000
15	2	14	←	14	2	13	43785.787	-0.042	1.000
15	1	15	←	14	1	14	41282.910	-0.016	1.000
15	1	14	←	14	1	13	44279.760	0.026	1.000
16	2	14	←	15	2	13	50120.695	-0.040	1.000
16	0	16	←	15	0	15	43968.612	0.001	1.000
16	2	15	←	15	2	14	46508.724	0.004	1.000
16	8	8	←	15	8	7	48912.097	0.028	1.000
16	10	7	←	15	10	6	48820.529	-0.003	1.000

Table 3.1 (Continued)

J_U	K_A	K_C		J_L	K_A	K_C	Obs / MHz	Obs-Calc	Weight
16	1	15	←	15	1	14	46871.295	-0.014	1.000
16	1	16	←	15	1	15	43950.828	0.009	1.000
17	3	14	←	16	3	13	54616.724	-0.046	1.000
17	0	17	←	16	0	16	46628.260	-0.033	1.000
17	2	16	←	16	2	15	49215.588	0.034	1.000
17	4	14	←	16	4	13	52340.126	-0.021	1.000
17	8	10	←	16	8	9	52003.471	0.035	1.000
17	1	16	←	16	1	15	49474.017	-0.017	1.000
17	1	17	←	16	1	16	46617.130	0.029	1.000
17	15	2	←	16	15	1	51785.774	0.016	1.000
17	13	5	←	16	13	4	51814.463	0.048	1.000
17	11	7	←	16	11	6	51859.828	-0.012	1.000
17	10	8	←	16	10	7	51893.505	0.047	1.000
17	9	9	←	16	9	8	51939.101	0.012	1.000
18	3	15	←	17	3	14	57745.967	-0.014	1.000
18	1	18	←	17	1	17	49282.353	0.017	1.000
18	3	16	←	17	3	15	54155.147	0.013	1.000
18	1	17	←	17	1	16	52089.654	-0.016	1.000
18	0	18	←	17	0	17	49289.321	0.002	1.000

Table 3.1 (Continued)

J_U	K_A	K_C		J_L	K_A	K_C	Obs / MHz	Obs-Calc	Weight
19	5	14	←	18	5	13	59218.637	0.027	1.000
19	2	18	←	18	2	17	54594.292	0.035	1.000
19	9	11	←	18	9	10	58115.384	0.001	1.000
19	17	2	←	18	17	1	57874.349	-0.018	1.000
19	1	19	←	18	1	18	51946.890	-0.013	1.000
19	1	18	←	18	1	17	54717.134	-0.003	1.000
19	0	19	←	18	0	18	51951.198	-0.031	1.000
20	5	15	←	19	5	14	62599.545	-0.046	1.000
20	5	16	←	19	5	15	61845.264	-0.014	1.000
20	1	19	←	19	1	18	57354.281	0.010	1.000
20	1	20	←	19	1	19	54611.056	0.006	1.000
20	2	19	←	19	2	18	57271.683	0.007	1.000
20	0	20	←	19	0	19	54613.730	0.015	1.000
20	9	12	←	19	9	11	61211.802	0.021	1.000
20	10	11	←	19	10	10	61137.045	0.002	1.000
20	11	10	←	19	11	9	61082.161	-0.005	1.000
20	12	9	←	19	12	8	61040.605	0.018	1.000
20	19	1	←	19	19	0	60908.355	0.041	1.000
20	15	5	←	19	15	4	60961.822	-0.022	1.000

Table 3.1 (Continued)

J_U	K_A	K_C		J_L	K_A	K_C	Obs / MHz	Obs-Calc	Weight
20	14	6	←	19	14	5	60982.624	0.022	1.000
20	13	8	←	19	13	7	61008.295	0.028	1.000
21	5	16	←	20	5	15	66041.523	0.011	1.000
21	1	20	←	20	1	19	59998.759	-0.040	1.000
21	2	20	←	20	2	19	59944.029	0.018	1.000
21	0	21	←	20	0	20	57276.573	0.003	1.000
21	3	19	←	20	3	18	62473.423	0.028	1.000
21	1	21	←	20	1	20	57274.942	0.004	1.000
21	3	18	←	20	3	17	66510.935	0.041	1.000
21	2	19	←	20	2	18	63105.160	0.019	1.000
21	19	2	←	20	19	1	63962.699	0.023	1.000
21	18	3	←	20	18	2	63974.443	-0.045	1.000
21	17	5	←	20	17	4	63988.321	-0.013	1.000
21	9	13	←	20	9	12	64314.131	-0.005	1.000
21	10	12	←	20	10	11	64227.333	-0.021	1.000
21	11	11	←	20	11	10	64163.684	-0.040	1.000
21	12	10	←	20	12	9	64115.515	-0.044	1.000
21	4	18	←	20	4	17	64300.845	-0.005	1.000
22	0	22	←	21	0	21	59939.664	0.002	1.000

Table 3.1 (Continued)

J_U	K_A	K_C		J_L	K_A	K_C	Obs / MHz	Obs-Calc	Weight
22	2	21	←	21	2	20	62612.831	0.015	1.000
22	1	21	←	21	1	20	62648.724	-0.027	1.000
22	3	20	←	21	3	19	65198.874	-0.033	1.000
22	15	8	←	21	15	7	67089.172	-0.032	1.000
22	14	9	←	21	14	8	67116.746	-0.022	1.000
22	13	10	←	21	13	9	67150.859	-0.033	1.000
22	12	11	←	21	12	10	67193.927	0.009	1.000
22	4	19	←	21	4	18	67203.159	0.012	1.000
22	11	12	←	21	11	11	67249.316	-0.038	1.000
22	1	22	←	21	1	21	59938.689	0.022	1.000
22	4	18	←	21	4	17	70809.116	0.023	1.000
23	5	18	←	22	5	17	73070.907	0.035	1.000
23	5	19	←	22	5	18	71141.543	0.029	1.000
23	4	20	←	22	4	19	70068.970	0.025	1.000
23	4	19	←	22	4	18	74009.119	-0.017	1.000
24	5	20	←	23	5	19	74187.249	-0.017	1.000
24	1	24	←	23	1	23	65265.866	-0.007	1.000
24	0	24	←	23	0	23	65266.235	-0.003	1.000
25	5	21	←	24	5	20	77199.171	-0.014	1.000

Table 3.1 (Continued)

J_U	K_A	K_C		J_L	K_A	K_C	Obs / MHz	Obs-Calc	Weight
25	14	12	←	24	14	11	76337.682	0.014	1.000
25	13	13	←	24	13	12	76387.761	-0.004	1.000
26	13	14	←	25	13	13	79473.450	0.024	1.000
26	15	12	←	25	15	11	79371.582	-0.010	1.000
26	23	3	←	25	23	2	79192.875	-0.046	1.000
26	19	7	←	25	19	6	79255.433	0.040	1.000
26	20	6	←	25	20	5	79236.452	0.035	1.000
26	16	10	←	25	16	9	79334.396	0.017	1.000
26	17	9	←	25	17	8	79303.476	0.002	1.000
26	21	5	←	25	21	4	79219.980	0.011	1.000
26	18	8	←	25	18	7	79277.476	-0.011	1.000
26	14	13	←	25	14	12	79417.018	-0.017	1.000

Table 3.2: Rotational and Determinable Quartic Centrifugal Distortion Constants for 2-Chloropyrimidine Isotopomers

	Normal Species	2-^{13}C	1,3-^{15}N	^{37}Cl
A_0 / MHz	6080.043(20)	6080.435(25)	5878.40(3)	6080.080(24)
B_0 / MHz	1705.7167(7)	1705.0289(16)	1705.2942(17)	1657.4396(14)
C_0 / MHz	1331.9569(6)	1331.5605(6)	1321.7568(10)	1302.3332(6)
D_J / kHz	0.0612(29)	0.0609(9)	0.0590(8)	0.0584(6)
D_{JK} / kHz	0.3386(6)	0.330(4)	0.332(3)	0.3217(11)
D_K / kHz	0.0 [a]	0.0 [a]	0.0 [a]	0.0[a]
d_1 / kHz	-0.0161(4)	-0.0160(7)	-0.0163(7)	-0.0150(5)
d_2 / kHz	-0.0031(2)	-0.0031(3)	-0.0014(4)	-0.0024(3)
Δ / amu Å^2	0.0195			

	2-^{13}C,^{37}Cl	1,3-^{15}N,^{37}Cl	4-^{13}C
A_0 / MHz	6080.60(25)	5878.33(5)	5981.22(6)
B_0 / MHz	1656.930(18)	1656.8703(19)	1692.081(4)
C_0 / MHz	1302.039(14)	1292.4771(13)	1318.8780(23)
D_J / kHz	0.056(7)	0.0569(13)	0.0642(19)
D_{JK} / kHz	0.325(17)	0.325(9)	0.0[a]
D_K / kHz	0.0[a]	0.0[a]	0.0[a]
d_1 / kHz	-0.013(8)	-0.0148(11)	-0.0177(17)
d_2 / kHz	0.0[a]	-0.0015(6)	0.0[a]

[a] Value fixed was not determinable from the data set

Table 3.3: Rotational Transitions of ^{37}Cl 2-Chloropyrimidine

J_u	K_A	K_C		J_l	K_A	K_C	Obs / MHz	Obs-Calc	Weight
13	2	11	←	12	2	10	40418.799	-0.011	1.000
13	1	12	←	12	1	11	38243.479	-0.007	1.000
14	1	14	←	13	1	13	37750.308	0.003	1.000
14	0	14	←	13	0	13	37801.329	-0.018	1.000
14	2	13	←	13	2	12	40092.748	0.019	1.000
14	1	13	←	13	1	12	40794.520	-0.031	1.000
15	2	13	←	14	2	12	46206.237	0.021	1.000
15	0	15	←	14	0	14	40395.753	0.013	1.000
15	1	15	←	14	1	14	40362.344	0.005	1.000
15	2	14	←	14	2	13	42780.887	-0.031	1.000
15	1	14	←	14	1	13	43328.543	-0.006	1.000
16	2	14	←	15	2	13	48965.742	-0.069	1.000
16	0	16	←	15	0	15	42993.259	-0.057	1.000
16	2	15	←	15	2	14	45449.624	0.047	1.000
16	1	16	←	15	1	15	42971.729	0.016	1.000
16	1	15	←	15	1	14	45861.385	-0.038	1.000
17	2	15	←	16	2	14	51637.214	-0.055	1.000
17	0	17	←	16	0	16	45593.115	-0.003	1.000
17	1	17	←	16	1	16	45579.279	-0.001	1.000

Table 3.3 (Continued)

J_U	K_A	K_C		J_L	K_A	K_C	Obs / MHz	Obs-Calc	Weight
17	1	16	←	16	1	15	48402.216	-0.114	1.000
18	5	13	←	17	5	12	54339.626	0.107	1.000
18	0	18	←	17	0	17	48194.477	0.038	1.000
18	2	17	←	17	2	16	50741.074	0.029	1.000
18	1	18	←	17	1	17	48185.639	-0.009	1.000
18	1	17	←	17	1	16	50954.802	-0.018	1.000
19	3	16	←	18	3	15	59242.541	0.005	1.000
19	0	19	←	18	0	18	50796.792	0.015	1.000
19	1	19	←	18	1	18	50791.233	0.001	1.000
20	4	16	←	19	4	15	62272.791	-0.028	1.000
20	3	17	←	19	3	16	62150.746	-0.172	0.000
20	3	18	←	19	3	17	58340.585	0.150	0.000
20	2	18	←	19	2	17	59276.453	0.055	1.000
21	4	17	←	20	4	16	65595.109	0.015	1.000
21	1	21	←	20	1	20	56001.099	0.023	1.000
21	3	18	←	20	3	17	64958.865	-0.026	1.000
21	2	19	←	20	2	18	61770.722	-0.024	1.000
21	0	21	←	20	0	20	56003.288	0.045	1.000
21	4	18	←	20	4	17	62711.205	0.041	1.000

Table 3.3 (Continued)

J_U	K_A	K_C		J_L	K_A	K_C	Obs / MHz	Obs-Calc	Weight
21	5	16	←	20	5	15	64104.620	0.127	0.000
22	4	18	←	21	4	17	68852.582	-0.046	1.000
22	2	21	←	21	2	20	61217.520	0.002	1.000
22	3	20	←	21	3	19	63712.595	-0.003	1.000
22	19	4	←	21	19	3	65284.187	0.011	1.000
22	18	5	←	21	18	4	65296.252	-0.063	1.000
22	17	6	←	21	17	5	65310.586	0.039	1.000
22	16	7	←	21	16	6	65327.403	-0.023	1.000
22	15	8	←	21	15	7	65347.751	0.054	1.000
22	14	8	←	21	14	7	65372.396	0.012	1.000
22	13	10	←	21	13	9	65402.921	-0.014	1.000
22	11	12	←	21	11	11	65491.010	-0.019	1.000
22	4	19	←	21	4	18	65564.003	0.025	1.000
23	3	20	←	22	3	19	70282.270	0.053	1.000
23	3	21	←	22	3	20	66369.619	-0.042	1.000
23	2	22	←	22	2	21	63825.951	0.025	1.000
23	11	13	←	22	11	12	68497.535	0.044	1.000
23	2	21	←	22	2	20	66781.492	-0.118	0.000
23	17	7	←	22	17	6	68291.296	0.004	1.000

Table 3.3 (Continued)

J_U	K_A	K_C		J_L	K_A	K_C	Obs / MHz	Obs-Calc	Weight
23	16	8	←	22	16	7	68310.586	0.048	1.000
23	15	8	←	22	15	7	68333.675	0.008	1.000
23	14	10	←	22	14	9	68361.832	-0.020	1.000
23	4	20	←	22	4	19	68382.844	-0.019	1.000
23	13	11	←	22	13	10	68396.738	-0.013	1.000
23	12	12	←	22	12	11	68440.783	0.018	1.000
24	4	20	←	23	4	19	75110.524	-0.035	1.000
24	1	23	←	23	1	22	66452.495	-0.012	1.000
24	3	22	←	23	3	21	69011.922	0.007	1.000
24	3	21	←	23	3	20	72822.410	0.035	1.000
24	2	22	←	23	2	21	69310.001	0.028	1.000
24	2	23	←	23	2	22	66432.394	-0.022	1.000
24	4	21	←	23	4	20	71168.445	0.012	1.000
24	19	5	←	23	19	4	71239.598	-0.012	1.000
24	17	7	←	23	17	6	71273.643	-0.007	1.000
24	15	9	←	23	15	8	71321.679	-0.049	1.000
24	14	11	←	23	14	10	71353.699	-0.034	1.000
24	13	12	←	23	13	11	71393.392	0.008	1.000
24	12	13	←	23	12	12	71443.449	0.025	1.000

Table 3.3 (Continued)

J_U	K_A	K_C		J_L	K_A	K_C	Obs / MHz	Obs-Calc	Weight
24	11	14	←	23	11	13	71507.988	0.018	1.000
25	4	21	←	24	4	20	78089.551	0.003	1.000
25	2	23	←	24	2	22	71854.237	0.001	1.000
25	3	22	←	24	3	21	75310.686	0.077	1.000
25	2	24	←	24	2	23	69037.632	-0.012	1.000
26	3	23	←	25	3	22	77772.410	0.199	0.000
26	2	24	←	25	2	23	74412.318	0.046	1.000
26	3	24	←	25	3	23	74264.109	-0.016	1.000
27	4	24	←	26	4	23	79345.282	-0.032	1.000
27	3	25	←	26	3	24	76879.083	-0.051	1.000
27	2	25	←	26	2	24	76981.453	0.008	1.000
27	2	26	←	26	2	25	74246.009	0.007	1.000
28	3	26	←	27	3	25	79489.317	-0.052	1.000
28	2	27	←	27	2	26	76849.644	-0.004	1.000
29	2	28	←	28	2	27	79453.138	-0.003	1.000

Table 3.4: Rotational Transitions of 2-^{13}C 2-Chloropyrimidine

J_U	K_A	K_C	←	J_L	K_A	K_C	Obs / MHz	Obs-Calc	Weight
14	2	12	←	13	2	11	44440.936	-0.020	1.000
14	1	13	←	13	1	12	41680.377	0.054	0.250
15	1	14	←	14	1	13	44267.100	0.011	0.000
15	3	13	←	14	3	12	45544.857	0.004	1.000
15	2	13	←	14	2	12	47322.178	0.015	1.000
16	1	16	←	15	1	15	43937.686	-0.022	1.000
16	0	16	←	15	0	15	43955.560	0.001	1.000
16	3	14	←	15	3	13	48442.985	0.008	1.000
16	2	15	←	15	2	14	46494.449	-0.004	1.000
16	2	14	←	15	2	13	50105.261	0.030	1.000
17	0	17	←	16	0	16	46614.466	0.028	1.000
17	3	15	←	16	3	14	51306.938	-0.005	1.000
17	1	16	←	16	1	15	49459.667	-0.071	0.250
17	2	16	←	16	2	15	49200.545	-0.030	1.000
17	1	17	←	16	1	16	46603.196	-0.010	1.000
18	3	15	←	17	3	14	57725.122	-0.014	1.000
18	1	18	←	17	1	17	49267.627	-0.027	1.000
18	0	18	←	17	0	17	49274.661	-0.004	1.000
19	1	19	←	18	1	18	51931.461	0.029	1.000

Table 3.4 (Continued)

J_U	K_A	K_C		J_L	K_A	K_C	Obs / MHz	Obs-Calc	Weight
19	0	19	←	18	0	18	51935.780	0.003	1.000
19	1	19	←	18	1	18	51931.464	0.032	1.000
19	3	17	←	18	3	16	56937.039	-0.002	1.000
19	4	16	←	18	4	15	58366.495	-0.010	1.000
19	3	16	←	18	3	15	60754.496	0.011	1.000
20	3	17	←	19	3	16	63677.025	0.011	1.000
20	4	17	←	19	4	16	61340.610	-0.015	1.000
20	3	18	←	19	3	17	59708.028	0.022	1.000
21	4	18	←	20	4	17	64279.060	0.022	1.000
21	3	18	←	20	3	17	66490.072	-0.032	1.000
21	3	19	←	20	3	18	62453.996	-0.025	1.000
22	3	20	←	21	3	19	65178.927	0.033	1.000
22	13	9	←	21	13	8	67126.528	-0.006	1.000
22	12	10	←	21	12	9	67169.478	-0.002	1.000
22	10	13	←	21	10	12	67297.997	0.005	1.000
22	11	12	←	21	11	11	67224.821	0.007	1.000
22	2	21	←	21	2	20	62594.113	-0.002	1.000
22	1	21	←	21	1	20	62630.192	-0.014	1.000
23	1	23	←	22	1	22	62583.656	-0.009	1.000

Table 3.4 (Continued)

J_U	K_A	K_C		J_L	K_A	K_C	Obs / MHz	Obs-Calc	Weight
23	0	23	←	22	0	22	62584.260	-0.012	1.000
24	0	24	←	23	0	23	65246.817	0.005	1.000
24	1	24	←	23	1	23	65246.448	0.003	1.000

Table 3.5: Rotational Transitions of 1,3-^{15}N 2-Chloropyrimidine

J_u	K_A	K_C		J_l	K_A	K_C	Obs / MHz	Obs-Calc	Weight
15	7	9	←	14	7	8	45765.511	0.100	1.000
15	8	8	←	14	8	7	45693.855	0.007	1.000
15	2	13	←	14	2	12	47046.476	-0.035	1.000
16	8	9	←	15	8	8	48773.538	0.033	1.000
16	9	8	←	15	9	7	48714.572	0.016	1.000
16	2	15	←	15	2	14	46178.397	-0.026	1.000
16	3	13	←	15	3	12	51319.540	-0.052	1.000
16	3	14	←	15	3	13	48204.090	-0.058	1.000
16	1	15	←	15	1	14	46476.036	-0.061	1.000
17	8	10	←	16	8	9	51859.813	0.054	1.000
17	9	9	←	16	9	8	51788.889	0.030	1.000
17	10	8	←	16	10	7	51738.632	0.008	1.000
17	11	7	←	16	11	6	51701.598	-0.041	1.000
17	2	16	←	16	2	15	48858.078	0.002	1.000
17	3	15	←	16	3	14	51033.863	0.004	1.000
17	1	16	←	16	1	15	49064.562	-0.049	1.000
17	0	17	←	16	0	16	46269.552	0.045	1.000
17	1	17	←	16	1	16	46261.164	-0.004	1.000
18	3	16	←	17	3	15	53829.274	-0.020	1.000

Table 3.5 (Continued)

J_U	K_A	K_C		J_L	K_A	K_C	Obs / MHz	Obs-Calc	Weight
18	2	17	←	17	2	16	51526.266	0.020	1.000
18	1	17	←	17	1	16	51666.303	-0.063	1.000
18	1	18	←	17	1	17	48905.624	0.018	1.000
19	3	16	←	18	3	15	60488.954	-0.043	1.000
19	1	19	←	18	1	18	51549.535	0.016	1.000
19	1	18	←	18	1	17	54279.293	0.012	1.000
19	0	19	←	18	0	18	51552.625	0.018	1.000
20	3	17	←	19	3	16	63321.157	0.020	1.000
20	0	20	←	19	0	19	54194.994	0.020	1.000
20	1	20	←	19	1	19	54193.135	0.022	1.000
20	3	18	←	19	3	17	59329.450	0.017	1.000
20	11	10	←	19	11	9	60903.287	0.022	1.000
20	10	11	←	19	10	10	60963.683	-0.010	1.000
20	4	17	←	19	4	16	61087.029	0.018	1.000
20	2	18	←	19	2	17	60010.014	0.042	1.000
21	9	13	←	20	9	12	64144.577	0.080	1.000
21	10	12	←	20	10	11	64048.776	-0.015	1.000
21	12	10	←	20	12	9	63925.664	-0.017	1.000
21	2	20	←	20	2	19	59489.016	0.004	1.000

Table 3.5 (Continued)

J_U	K_A	K_C		J_L	K_A	K_C	Obs / MHz	Obs-Calc	Weight
21	4	18	←	20	4	17	63986.051	0.006	1.000
21	3	18	←	20	3	17	66039.919	0.085	1.000
21	1	20	←	20	1	19	59528.705	0.000	1.000
21	4	17	←	20	4	16	67461.261	0.039	1.000
21	11	11	←	20	11	10	63978.656	-0.041	1.000
21	3	19	←	20	3	18	62041.905	-0.003	1.000
22	11	12	←	21	11	11	67058.594	-0.034	1.000
22	12	11	←	21	12	10	66997.563	-0.027	1.000
22	11	12	←	21	11	11	67058.602	-0.026	1.000
22	10	13	←	21	10	12	67139.424	0.002	1.000
22	4	18	←	21	4	17	70681.004	-0.079	1.000
22	2	21	←	21	2	20	62135.651	0.005	1.000
22	4	19	←	21	4	18	66846.081	0.011	1.000
22	1	21	←	21	1	20	62161.041	-0.049	1.000
22	2	20	←	21	2	19	65094.802	-0.105	1.000
22	12	11	←	21	12	10	66997.571	-0.019	1.000
22	3	19	←	21	3	18	68658.782	0.011	1.000
23	1	22	←	22	1	21	64796.596	-0.017	1.000
23	3	20	←	22	3	19	71202.575	0.073	1.000
23	14	10	←	22	14	9	69976.466	0.054	1.000

Table 3.5 (Continued)

J_U	K_A	K_C		J_L	K_A	K_C	Obs / MHz	Obs-Calc	Weight
23	13	11	←	22	13	10	70019.258	-0.035	1.000
23	2	21	←	22	2	20	67664.823	-0.037	1.000
23	11	13	←	22	11	12	70143.305	0.007	1.000
23	4	20	←	22	4	19	69668.383	0.009	1.000
23	12	12	←	22	12	11	70073.442	0.010	1.000
23	3	21	←	22	3	20	67412.576	-0.016	1.000
23	2	22	←	22	2	21	64780.465	0.010	1.000
24	2	22	←	23	2	21	70251.923	-0.038	1.000
24	2	23	←	23	2	22	67424.111	-0.007	1.000
24	3	22	←	23	3	21	70078.525	0.033	1.000
24	1	23	←	23	1	22	67434.306	0.010	1.000
25	3	23	←	24	3	22	72735.728	0.005	1.000
25	2	24	←	24	2	23	70067.075	-0.016	1.000
25	1	24	←	24	1	23	70073.463	0.007	1.000
25	2	23	←	24	2	22	72853.196	0.061	1.000
25	1	24	←	24	1	23	70073.459	0.003	1.000
26	2	25	←	25	2	24	72709.648	-0.023	1.000

Table 3.6: Rotational Transitions of 2-^{13}C,^{37}Cl- 2-Chloropyrimidine

J_u	K_A	K_C		J_l	K_A	K_C	Obs / MHz	Obs-Calc	Weight
19	4	16	←	18	4	15	56891.532	0.067	1.000
19	2	17	←	18	2	16	56758.714	0.004	1.000
19	3	16	←	18	3	15	59226.582	-0.124	1.000
20	3	18	←	19	3	17	58326.538	0.082	1.000
20	11	10	←	19	11	9	59473.029	0.065	1.000
20	4	16	←	19	4	15	62253.292	0.129	1.000
20	3	17	←	19	3	16	62135.188	0.121	1.000
21	11	11	←	20	11	10	62471.194	0.072	1.000
21	1	20	←	20	1	19	58662.353	-0.006	1.000
21	12	10	←	20	12	9	62428.046	-0.038	1.000
21	13	9	←	20	13	8	62394.602	-0.037	1.000
21	3	19	←	20	3	18	61022.851	-0.046	1.000
21	4	18	←	20	4	17	62694.679	-0.198	1.000
21	4	17	←	20	4	16	65574.930	0.056	1.000
21	3	18	←	20	3	17	64943.134	-0.002	1.000
22	1	21	←	21	1	20	61250.097	0.035	1.000
22	3	19	←	21	3	18	67651.050	-0.009	1.000
22	11	12	←	21	11	11	65472.990	0.079	1.000
22	2	20	←	21	2	19	64255.973	0.026	1.000

Table 3.6 (Continued)

J_u	K_A	K_C		J_l	K_A	K_C	Obs / MHz	Obs-Calc	Weight
22	12	11	←	21	12	10	65423.347	-0.041	1.000
22	13	10	←	21	13	9	65385.000	0.068	1.000
22	4	19	←	21	4	18	65547.263	0.031	1.000
22	2	21	←	21	2	20	61203.750	0.093	1.000
22	3	20	←	21	3	19	63697.797	0.112	1.000
23	2	21	←	22	2	20	66767.276	-0.030	1.000
23	3	20	←	22	3	19	70266.731	-0.028	1.000
23	11	13	←	22	11	12	68478.497	-0.021	1.000
23	4	20	←	22	4	19	68365.764	0.074	1.000
23	4	19	←	22	4	18	72007.720	-0.130	1.000
23	3	21	←	22	3	20	66354.397	0.130	1.000
23	2	22	←	22	2	21	63811.581	0.084	1.000
23	13	11	←	22	13	10	68377.937	0.027	1.000
23	1	22	←	22	1	21	63842.288	0.065	1.000
23	12	12	←	22	12	11	68421.860	-0.007	1.000
23	14	9	←	22	14	8	68343.143	0.089	1.000
24	3	22	←	23	3	21	68996.113	0.089	1.000
24	3	21	←	23	3	20	72807.072	0.135	1.000
24	4	21	←	23	4	20	71150.943	0.090	1.000

Table 3.6 (Continued)

J_u	K_A	K_C		J_l	K_A	K_C	Obs / MHz	Obs-Calc	Weight
24	11	14	←	23	11	13	71488.146	0.009	1.000
24	12	13	←	23	12	12	71423.673	-0.004	1.000
24	2	22	←	23	2	21	69294.921	-0.043	1.000
24	2	23	←	23	2	22	66417.506	0.092	1.000
24	13	12	←	23	13	11	71373.717	0.015	1.000
24	1	23	←	23	1	22	66437.634	0.052	1.000
25	2	24	←	24	2	23	69022.132	0.066	1.000
25	2	23	←	24	2	22	71838.562	0.042	1.000
25	1	25	←	24	1	24	66403.820	-0.081	1.000
26	1	25	←	25	1	24	71634.514	0.101	1.000

Table 3.7: Rotational Transitions of 1,3-^{15}N,^{37}Cl- 2-Chloropyrimidine

J_u	K_A	K_C		J_l	K_A	K_C	Obs / MHz	Obs-Calc	Weight
15	8	8	←	14	8	7	44497.796	0.009	1.000
15	9	7	←	14	9	6	44454.450	0.010	1.000
15	2	13	←	14	2	12	45945.692	-0.036	1.000
16	8	9	←	15	8	8	47494.188	0.042	1.000
16	9	8	←	15	9	7	47441.424	-0.022	1.000
16	2	14	←	15	2	13	48640.004	-0.024	1.000
17	3	14	←	16	3	13	53038.086	-0.030	1.000
17	3	15	←	16	3	14	49817.228	0.020	1.000
17	1	17	←	16	1	16	45235.546	-0.027	1.000
17	8	10	←	16	8	9	50496.392	0.008	1.000
17	9	9	←	16	9	8	50433.009	-0.015	1.000
17	10	8	←	16	10	7	50388.160	0.061	1.000
17	1	16	←	16	1	15	48003.301	0.037	1.000
17	2	16	←	16	2	15	47759.721	0.013	1.000
17	0	17	←	16	0	16	45246.005	-0.009	1.000
17	2	15	←	16	2	14	51246.559	0.056	1.000
18	3	16	←	17	3	15	52562.733	-0.013	1.000
18	9	10	←	17	9	9	53429.476	-0.010	1.000
18	1	18	←	17	1	17	47821.791	0.031	1.000

Table 3.7 (Continued)

J_u	K_A	K_C		J_l	K_A	K_C	Obs / MHz	Obs-Calc	Weight
18	0	18	←	17	0	17	47828.267	0.012	1.000
18	10	9	←	17	10	8	53376.090	0.014	1.000
18	11	8	←	17	11	7	53336.702	-0.071	1.000
18	1	17	←	17	1	16	50542.192	-0.018	1.000
18	2	17	←	17	2	16	50373.273	0.008	1.000
19	2	18	←	18	2	17	52977.657	0.047	1.000
19	1	18	←	18	1	17	53092.609	0.026	1.000
19	1	19	←	18	1	18	50407.298	-0.022	1.000
19	0	19	←	18	0	18	50411.323	-0.009	1.000
20	1	20	←	19	1	19	52992.464	-0.024	1.000
20	0	20	←	19	0	19	52994.915	-0.037	1.000
21	11	11	←	20	11	10	62303.258	-0.034	1.000
21	2	19	←	20	2	18	61223.803	0.015	1.000
22	3	19	←	21	3	18	67166.794	0.037	1.000
22	1	21	←	21	1	20	60790.714	0.007	1.000
22	2	20	←	21	2	19	63709.961	-0.031	1.000
23	1	22	←	22	1	21	63366.191	0.007	1.000
23	3	21	←	22	3	20	65898.344	-0.005	1.000
23	2	21	←	22	2	20	66213.061	-0.096	1.000

Table 3.7 (Continued)

J_u	K_A	K_C		J_l	K_A	K_C	Obs / MHz	Obs-Calc	Weight
23	11	13	←	22	11	12	68300.697	0.006	1.000
23	12	12	←	22	12	11	68238.266	0.029	1.000
23	2	22	←	22	2	21	63344.615	-0.008	1.000
24	1	23	←	23	1	22	65944.222	-0.005	1.000
24	2	22	←	23	2	21	68733.457	-0.017	1.000
24	2	23	←	23	2	22	65930.386	0.004	1.000
25	1	24	←	24	1	23	68524.128	0.078	1.000
25	2	24	←	24	2	23	68515.218	-0.008	1.000

Table 3.8: Rotational Transitions of 2-Chloropyrimidine in the C–Cl Out of Plane Bend v=1 State

J_u	K_A	K_C		J_l	K_A	K_C	Obs / MHz	Obs-Calc	Weight
16	2	14	←	15	2	13	50154.875	-0.056	1.000
16	2	15	←	15	2	14	46555.027	0.004	1.000
16	1	15	←	15	1	14	46911.815	-0.022	1.000
16	1	16	←	15	1	15	44004.349	-0.025	1.000
16	0	16	←	15	0	15	44021.796	0.006	1.000
17	2	15	←	16	2	14	52847.854	0.023	1.000
17	0	17	←	16	0	16	46685.163	-0.005	1.000
17	2	16	←	16	2	15	49264.898	0.030	1.000
17	1	16	←	16	1	15	49518.757	-0.002	1.000
17	1	17	←	16	1	16	46674.236	0.008	1.000
18	1	18	←	17	1	17	49343.045	-0.008	1.000
18	2	17	←	17	2	16	51962.242	0.077	1.000
18	1	17	←	17	1	16	52138.612	0.011	1.000
18	0	18	←	17	0	17	49349.857	-0.011	1.000
18	1	17	←	17	1	16	52138.609	0.008	1.000
19	4	16	←	18	4	15	58443.277	-0.009	1.000
19	1	18	←	18	1	17	54770.219	0.014	1.000
19	4	15	←	18	4	14	60759.516	0.087	1.000
19	3	16	←	18	3	15	60822.342	-0.102	1.000

Table 3.8 (Continued)

J_u	K_A	K_C		J_l	K_A	K_C	Obs / MHz	Obs-Calc	Weight
19	0	19	←	18	0	18	52015.407	-0.030	1.000
19	1	19	←	18	1	18	52011.190	-0.030	1.000
19	0	19	←	18	0	18	52015.406	-0.031	1.000
20	4	16	←	19	4	15	64201.005	-0.019	1.000
20	2	19	←	19	2	18	57330.747	0.082	1.000
20	3	18	←	19	3	17	59781.034	-0.020	1.000
20	1	20	←	19	1	19	54678.983	0.008	1.000
20	4	16	←	19	4	15	64201.007	-0.017	1.000
20	3	17	←	19	3	16	63743.199	0.000	1.000
20	5	16	←	19	5	15	61909.617	-0.029	1.000
20	0	20	←	19	0	19	54681.578	0.010	1.000
20	12	9	←	19	12	8	61105.195	-0.004	1.000
20	13	8	←	19	13	7	61072.763	-0.003	1.000
20	14	7	←	19	14	6	61047.018	0.007	1.000
20	4	17	←	19	4	16	61419.741	-0.019	1.000
20	1	20	←	19	1	19	54678.984	0.008	1.000
21	3	19	←	20	3	18	62530.083	-0.007	1.000
21	4	18	←	20	4	17	64360.334	-0.009	1.000
21	4	17	←	20	4	16	67580.293	0.006	1.000

Table 3.8 (Continued)

J_u	K_A	K_C		J_l	K_A	K_C	Obs / MHz	Obs-Calc	Weight
21	2	20	←	20	2	19	60006.438	0.040	1.000
21	13	9	←	20	13	8	64145.980	0.039	1.000
21	12	10	←	20	12	9	64183.490	0.004	1.000
21	5	17	←	20	5	16	65031.990	-0.028	1.000
21	3	18	←	20	3	17	66554.401	0.100	1.000
22	12	11	←	21	12	10	67265.214	0.041	1.000
22	2	21	←	21	2	20	62678.745	0.084	1.000
22	13	10	←	21	13	9	67221.950	-0.044	1.000
22	3	20	←	21	3	19	65258.088	-0.074	1.000
22	14	8	←	21	14	7	67187.726	-0.024	1.000
22	4	19	←	21	4	18	67264.175	0.078	1.000
22	15	7	←	21	15	6	67160.090	0.000	1.000
23	3	21	←	22	3	20	67968.996	-0.116	1.000

Table 3.9: Rotational Transitions of 2-Chloropyrimidine in the C-Cl In-plane Bend v=1 State

J_u	K_A	K_C		J_l	K_A	K_C	Obs / MHz	Obs-Calc	Weight
13	2	11	←	12	2	10	41471.686	0.020	1.000
14	2	12	←	13	2	11	44449.573	0.034	1.000
14	2	13	←	13	2	12	41026.167	0.021	1.000
15	2	13	←	14	2	12	47330.908	0.079	1.000
15	2	14	←	14	2	13	43767.068	0.034	1.000
16	2	14	←	15	2	13	50113.591	-0.056	1.000
17	1	16	←	16	1	15	49454.106	-0.043	1.000
17	2	16	←	16	2	15	49193.194	-0.020	1.000
18	2	17	←	17	2	16	51885.482	-0.012	1.000
18	1	17	←	17	1	16	52067.267	-0.006	1.000
18	0	18	←	17	0	17	49255.666	0.002	1.000
18	1	18	←	17	1	17	49248.619	0.022	1.000
19	3	16	←	18	3	15	60767.446	-0.140	1.000
19	1	19	←	18	1	18	51911.017	0.005	1.000
19	0	19	←	18	0	18	51915.368	-0.025	1.000
20	12	9	←	19	12	8	61019.360	0.009	1.000
20	0	20	←	19	0	19	54575.708	0.007	1.000
20	1	20	←	19	1	19	54573.026	0.024	1.000

Table 3.9: (Continued)

J_u	K_A	K_C		J_l	K_A	K_C	Obs / MHz	Obs-Calc	Weight
13	2	11	←	12	2	10	41471.686	0.020	1.000
20	3	17	←	19	3	16	63690.638	-0.025	1.000
21	5	16	←	20	5	15	66018.827	0.006	1.000
21	3	18	←	20	3	17	66504.036	0.097	1.000
21	3	19	←	20	3	18	62451.423	-0.009	1.000
22	14	9	←	21	14	8	67093.389	-0.038	1.000
22	12	11	←	21	12	10	67170.661	0.040	1.000
22	3	20	←	21	3	19	65175.256	-0.085	1.000
22	13	10	←	21	13	9	67127.571	0.003	1.000
22	4	18	←	21	4	17	70796.064	0.011	1.000
23	4	20	←	22	4	19	70048.776	0.040	1.000
23	5	19	←	22	5	18	71120.858	0.014	1.000
23	5	18	←	22	5	17	73047.339	-0.017	1.000
24	4	21	←	23	4	20	72878.566	0.023	1.000

Table 3.10: Rotational Transitions of 2-Chloropyrimidine in a Ring Bending v=1 State

J_u	K_A	K_C		J_l	K_A	K_C	Obs / MHz	Obs-Calc	Weight
14	1	13	←	13	1	12	41709.512	-0.052	1.000
15	2	14	←	14	2	13	43805.122	-0.019	1.000
15	2	13	←	14	2	12	47351.680	-0.029	1.000
15	1	14	←	14	1	13	44298.791	-0.025	1.000
16	3	13	←	15	3	12	51410.385	0.028	1.000
16	3	14	←	15	3	13	48476.888	0.030	1.000
16	2	14	←	15	2	13	50136.821	0.128	1.000
16	2	15	←	15	2	14	46529.653	0.016	1.000
16	0	16	←	15	0	15	43993.254	-0.013	1.000
16	1	16	←	15	1	15	43975.460	-0.012	1.000
17	3	14	←	16	3	13	54630.460	-0.008	1.000
17	3	15	←	16	3	14	51342.969	0.029	1.000
17	1	17	←	16	1	16	46643.564	0.157	1.000
17	0	17	←	16	0	16	46654.574	-0.028	1.000
17	1	16	←	16	1	15	49496.495	-0.037	1.000
18	1	18	←	17	1	17	49310.292	-0.001	1.000
18	0	18	←	17	0	17	49317.289	0.010	1.000
18	1	17	←	17	1	16	52113.853	0.017	1.000
19	3	16	←	18	3	15	60791.736	-0.163	1.000

Table 3.10: (Continued)

J_u	K_A	K_C		J_l	K_A	K_C	Obs / MHz	Obs-Calc	Weight
19	1	18	←	18	1	17	54742.942	-0.013	1.000
19	1	19	←	18	1	18	51976.470	-0.041	1.000
19	1	19	←	18	1	18	51976.467	-0.044	1.000
19	0	19	←	18	0	18	51980.802	-0.038	1.000
19	2	18	←	18	2	17	54620.071	0.013	1.000
20	5	15	←	19	5	14	62616.904	-0.221	1.000
20	5	16	←	19	5	15	61864.819	0.007	1.000
20	13	8	←	19	13	7	61029.102	-0.058	1.000
20	1	20	←	19	1	19	54642.329	0.019	1.000
20	1	20	←	19	1	19	54642.329	0.019	1.000
20	1	19	←	19	1	18	57381.720	-0.011	1.000
20	4	16	←	19	4	15	64146.966	0.148	1.000
21	5	16	←	20	5	15	66059.444	0.126	1.000
21	5	17	←	20	5	16	64985.929	0.018	1.000
21	3	18	←	20	3	17	66530.832	0.039	1.000
21	1	21	←	20	1	20	57307.850	0.002	1.000
21	13	9	←	20	13	8	64100.119	0.060	1.000
21	0	21	←	20	0	20	57309.499	0.018	1.000
22	5	17	←	21	5	16	69555.772	-0.069	1.000

Table 3.10: (Continued)

J_u	K_A	K_C		J_l	K_A	K_C	Obs / MHz	Obs-Calc	Weight
22	4	19	←	21	4	18	67226.661	-0.036	1.000
22	3	20	←	21	3	19	65225.822	-0.013	1.000
22	5	18	←	21	5	17	68087.586	0.049	1.000

Table 3.11: Rotational Transitions of 2-Chloropyrimidine in the Out-of-Plane Bend v=2 State

J_u	K_A	K_C		J_l	K_A	K_C	Obs / MHz	Obs-Calc	Weight
15	2	13	←	14	2	12	47405.792	0.107	0.000
15	2	14	←	14	2	13	43872.393	0.001	1.000
15	1	14	←	14	1	13	44352.618	-0.002	1.000
16	0	16	←	15	0	15	44074.577	-0.026	1.000
16	1	16	←	15	1	15	44057.561	0.012	1.000
17	2	16	←	16	2	15	49313.905	0.008	1.000
17	0	17	←	16	0	16	46741.635	-0.016	1.000
17	1	16	←	16	1	15	49563.333	-0.002	1.000
17	1	17	←	16	1	16	46730.976	0.021	1.000
18	2	17	←	17	2	16	52014.288	-0.013	1.000
18	1	18	←	17	1	17	49403.342	-0.006	1.000
18	0	18	←	17	0	17	49410.041	0.038	1.000
18	1	17	←	17	1	16	52187.354	0.008	1.000
19	1	19	←	18	1	18	52075.074	-0.022	1.000
19	0	19	←	18	0	18	52079.198	-0.010	1.000
19	1	18	←	18	1	17	54823.051	0.001	1.000
20	1	20	←	19	1	19	54746.449	0.007	1.000
20	0	20	←	19	0	19	54748.967	0.000	1.000

Table 3.12: Rotational Transitions of 2-Chloropyrimidine in a Ring Bending v=1 State

J_u	K_A	K_C		J_l	K_A	K_C	Obs / MHz	Obs-Calc	Weight
15	2	13	←	14	2	12	47340.679	-0.029	1.000
15	1	14	←	14	1	13	44290.651	0.046	1.000
16	2	15	←	15	2	14	46518.944	-0.032	1.000
16	0	16	←	15	0	15	43983.035	0.047	1.000
16	1	16	←	15	1	15	43965.080	0.008	1.000
17	0	17	←	16	0	16	46643.570	-0.084	1.000
17	1	17	←	16	1	16	46632.358	-0.019	1.000
17	1	16	←	16	1	15	49486.778	-0.050	1.000
18	1	18	←	17	1	17	49298.616	-0.015	1.000
18	1	17	←	17	1	16	52103.369	0.039	1.000
18	0	18	←	17	0	17	49305.675	0.003	1.000
19	0	19	←	18	0	18	51968.634	0.054	1.000
19	1	18	←	18	1	17	54731.670	0.010	1.000
19	1	19	←	18	1	18	51964.257	0.043	1.000
20	1	20	←	19	1	19	54629.373	-0.005	1.000
20	0	20	←	19	0	19	54632.050	-0.018	1.000
21	4	17	←	20	4	16	67502.879	0.076	1.000
22	4	19	←	21	4	18	67209.236	-0.035	1.000
22	5	17	←	21	5	16	69526.109	-0.041	1.000

Table 3.13: Rotational and Determinable Quartic Centrifugal Distortion Constants for Measured Excited Vibrational States of 2-Chloropyrimidine

Parameter	State A	State B	State C	State 2A	State D
A / MHz	6054.29(5)	6101.27(6)	6075.30(8)	6029.12(8)	6079.72(5)
B / MHz	1707.077(5)	1705.709(4)	1705.954(5)	1708.446(8)	1705.363(8)
C / MHz	1333.7742(22)	1330.8825(31)	1332.7861(31)	1335.575(16)	1332.453(3)
D_J / kHz	0.0615(22)	0.0596(15)	0.0582(26)	0.087(6)	0.065(4)
D_{JK} / kHz	0.336(3)	0.325(5)	0.343(9)	0.0[a]	0.0 [a]
D_K / kHz	0.0[a]	0.0[a]	0.0[a]	0.0[a]	0.0[a]
d_1 / kHz	-0.0131(21)	-0.1230(21)	-0.0102(25)	-0.0264(37)	-0.018(3)
d_2 / kHz	-0.0006(6)	-0.0016(7)	0.0014(11)	0.0[a]	0.0[a]
Δ / amu Å^2	-0.6149	0.6137	-0.2402	-1.237	-0.1876

[a] value held fixed

Table 3.14 : Rotational Transitions of 4-^{13}C-2-Chloropyrimidine

J_u	K_A	K_C		J_l	K_A	K_C	Obs / MHz	Obs-Calc	Weight
15	3	12	←	14	3	11	47713.126	0.090	1.000
16	2	14	←	15	2	13	49636.926	-0.040	1.000
16	2	15	←	15	2	14	46058.937	0.059	0.000
16	1	16	←	15	1	15	43519.928	0.168	0.000
16	3	14	←	15	3	13	48012.854	-0.043	1.000
16	1	15	←	15	1	14	46401.989	0.165	0.000
17	3	15	←	16	3	14	50846.298	-0.010	1.000
17	1	17	←	16	1	16	46159.684	-0.036	0.000
17	0	17	←	16	0	16	46170.030	-0.020	0.000
18	3	16	←	17	3	15	53646.386	-0.017	1.000
18	1	18	←	17	1	17	48798.719	0.026	1.000
18	0	18	←	17	0	17	48805.122	0.017	1.000
18	2	17	←	17	2	16	51403.909	0.068	1.000
18	1	17	←	17	1	16	51571.824	0.007	1.000
19	0	19	←	18	0	18	51441.012	0.017	1.000
19	1	18	←	18	1	17	54174.884	-0.026	0.000
19	2	18	←	18	2	17	54060.759	-0.144	0.000
19	2	17	←	18	2	16	57417.563	-0.180	1.000

Table 3.14 (Continued)

J_u	K_A	K_C		J_l	K_A	K_C	Obs / MHz	Obs-Calc	Weight
19	3	16	←	18	3	15	60227.227	0.036	1.000
19	4	15	←	18	4	14	60222.801	0.141	1.000
19	4	16	←	18	4	15	57866.537	-0.045	1.000
20	0	20	←	19	0	19	54077.477	0.051	0.000
20	2	19	←	19	2	18	56711.261	0.085	0.000
20	4	16	←	19	4	15	63627.847	-0.170	1.000
20	4	17	←	19	4	16	60808.937	-0.032	1.000
21	3	19	←	20	3	18	61872.562	0.004	1.000
21	3	18	←	20	3	17	65872.467	0.116	1.000
21	4	17	←	20	4	16	66967.646	-0.041	1.000
21	1	21	←	20	1	20	56712.735	0.004	1.000
22	4	18	←	21	4	17	70221.150	-0.131	0.000
22	1	21	←	21	1	20	62031.530	-0.013	1.000
22	4	19	←	21	4	18	66584.038	-0.040	0.000
22	3	20	←	21	3	19	64568.398	0.050	1.000
22	2	21	←	21	2	20	61998.852	0.076	1.000
22	4	19	←	21	4	18	66584.049	-0.029	1.000
23	1	23	←	22	1	22	61987.765	-0.045	1.000
23	2	22	←	22	2	21	64638.744	0.042	1.000

Table 3.14 (Continued)

J_u	K_A	K_C		J_l	K_A	K_C	Obs / MHz	Obs-Calc	Weight
23	1	22	←	22	1	21	64659.926	0.057	1.000
23	4	20	←	22	4	19	69416.527	0.009	1.000
23	0	23	←	22	0	22	61988.300	-0.050	1.000
24	4	21	←	23	4	20	72214.070	-0.002	1.000
24	3	21	←	23	3	20	73635.488	0.003	1.000
24	0	24	←	23	0	23	64625.520	-0.060	1.000
25	1	24	←	24	1	23	69923.365	-0.039	1.000
25	3	23	←	24	3	22	72569.474	0.013	1.000
25	4	22	←	24	4	21	74979.464	0.017	1.000
26	2	25	←	25	2	24	72551.844	0.012	1.000
26	3	24	←	25	3	23	75217.826	-0.375	0.000
26	1	25	←	25	1	24	72557.290	0.012	1.000

3.1.2 Molecular Structure

With the availability of a large number of rotational constants for a variety of isotopic species of 2-chloropyrimidine, it was possible to obtain a partial substitution structure for the heavy atoms in the molecule. For nuclei far from the a inertial axis, the method of single substitution was used. The nitrogen and 2-carbon centers lie rather close to the a inertial axis, and thus the method of double isotopic substitution was used to determine the a substitution coordinate for these nuclei. The b coordinates given for hydrogen represent those obtained from the first and second moments ($\sum m_i r_i = 0$ and $\sum m_i r_i^2 = I_b$) of the normal species. Errors in the substitution coordinates were arbitrarily assigned to the recommended value of 0.0012 Å[6], and the values with their errors are given in Table 3.15. The derivable bond length and angle parameters were calculated, along with the standard errors in each internal coordinate (Table 3.16).

It was also possible to arrive at a partial ground state r_0 structure for 2-chloropyrimidine. The refinement was carried out using iterative least squares with the C–H bond lengths held constant at the values previously obtained for fluorobenzene. The present r_0 structural refinement required several iterations to reach the convergence criteria, suggesting that the derived parameters are perhaps not reliable. The ground state geometrical parameters are given in Table 3.17. With the addition of rotational data for deuterated species of 2-chloropyrimidine, this large uncertainty should be ameliorated.

Table 3.15: Substitution Coordinates of 2-Chloropyrimidine[a]

atom	a	b
Cl	2.097(1)	0.0
C(2)	0.3772(12)	0.0
N(1)	-0.2033(12)	1.207(1)
N(3)	-0.2033(12)	-1.207(1)
C(4)	-1.5444(12)	-1.1817(12)
C(6)	-1.5444(12)	1.1817(12)
H(4)		-2.106
H(6)		2.106

[a] Coordinates are given in angstroms

Table 3.16: Determinable Substitution Bond Parameters in 2-Chloropyrimidine

Parameter	Value / Å	Parameter	Value / Degrees
r_{C-Cl}	1.720(6)	θ_{ClCN}	115.7(23)
$r_{C(2)-N}$	1.339(27)	θ_{CNC}	114.6(20)
$r_{N-C(4)}$	1.341(23)		

Table 3.17: Ground State Geometry of 2-Chloropyrimidine

Parameter	Value / Å	Parameter	Value / Degrees
r_{C-Cl}	1.702(4)	θ_{ClCN}	115.7(23)
$r_{C(2)-N}$	1.3546(29)	θ_{CNC}	114.6(20)
$r_{N-C(4)}$	1.3114(30)	θ_{NCH}	
r_{C-C}	1.391(3)		
$r_{C(4)-H}$	1.084(5)		
$r_{C(5)-H}$	1.077[a]		

[a] value held fixed

3.1.3 Chlorine Quadrupole Coupling Constants

As mentioned previously, significant hyperfine structure due to the presence of the chlorine nucleus was noticeable in transitions having high values of K_A. At large values of J, any structure due to the presence of the equivalent nitrogen nuclei within the ring had coalesced, giving considerable simplification to the observed spectrum. Assignment of the hyperfine components within a rotational transition was accomplished by transferrence of the previously measured coupling constants of chlorobenzene together with predictions of splittings from standard formulae [1]. In most cases, the quadrupole structure was resolvable into doublets, and for transitions lower in J it was possible to observe quartets (Figure 3.1). By contrast, low K_A lines showed no resolvable hyperfine structure (Figure 3.2). From the assigned hyperfine components it was possible to obtain least squares values for the diagonal

elements of the chlorine quadrupole coupling tensor in the principal inertial axes. Some experimentally measured frequencies of resolved components are given in Table 3.18 with obtainable values of quadrupole coupling constants included in Table 3.19. A total of 38 splittings were included in the least squares fit of the normal species.

Hyperfine components were measured for six isotopic species of 2-chloropyrimidine, with least squares calculations giving a good value of χ_{aa} in all cases. Determination of the asymmetry of the coupling tensor was made difficult by the fact that the molecule has only a-type transitions. This problem could not be overcome by extending measurements to lower J values, as Nitrogen hyperfine structure then becomes apparent and complicates the observed patterns. The ratio of the principal coupling constants observed in the normal species and the ^{37}Cl containing species is determined as 1.273, consistent with the ratio of the quadrupole moments of the two nuclei (1.270) [8], further confirming the assignment of the ^{37}Cl species. Least squares values of the principal element and asymmetry of the chlorine quadrupole coupling tensor are summarized in Table 3.19 for the measured isotopic species.

3.2 2-Fluoropyrimidine

Analogous to 2-chloropyrimidine, 2-fluoropyrimidine showed a strong a-type spectrum, making the assignment less complicated, as again low K_A lines could be tuned out by using low Stark modulation fields to obtain values of B and C. The value of A was determined by extending the search to lower values of K_A. Observed rotational transitions and derived rotational constants of 2-fluoropyrimidine will be given in a later communication.

Table 3.18: Some Examples of Observed Hyperfine Splittings in ^{35}Cl-2-Chloropyrimidine in MHz

J_U	K_A	K_C	-	J_L	K_A	K_C	F_U	-	F_L	Obs	Obs - Calc
13	12	2	←	12	12	1				39596.639	
							$\frac{27}{2}$	←	$\frac{25}{2}$	39592.533	0.052
							$\frac{25}{2}$	←	$\frac{23}{2}$	39593.574	-0.095
							$\frac{29}{2}$	←	$\frac{27}{2}$	39599.677	0.036
							$\frac{23}{2}$	←	$\frac{21}{2}$	39600.772	-0.024
14	13	1	←	13	13	0				42641.336	
							$\frac{29}{2}$	←	$\frac{27}{2}$	42637.533	-0.026
							$\frac{27}{2}$	←	$\frac{25}{2}$	42638.453	-0.051
							$\frac{31}{2}$	←	$\frac{29}{2}$	42644.202	-0.049
							$\frac{25}{2}$	←	$\frac{23}{2}$	42645.156	-0.040
20	19	1	←	19	19	0				60908.355	
							$\frac{41}{2}$	←	$\frac{39}{2}$	60905.670	-0.014
							$\frac{39}{2}$	←	$\frac{37}{2}$	60906.132	-0.036
							$\frac{43}{2}$	←	$\frac{41}{2}$	60910.562	-0.011
							$\frac{37}{2}$	←	$\frac{35}{2}$	60911.055	-0.002

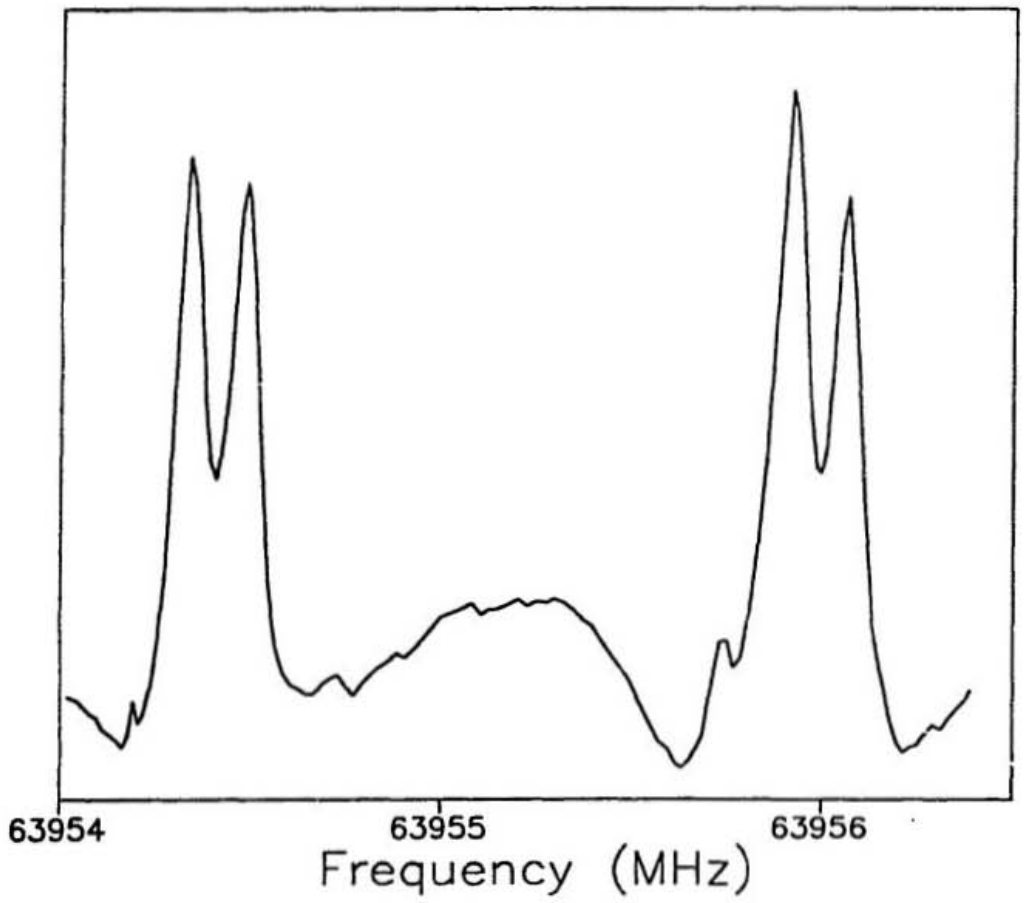

Figure 3.1: Hyperfine Components of the $21_{19,2} \leftarrow 20_{18,2}$ Rotational Transition of 2-Chloropyrimidine

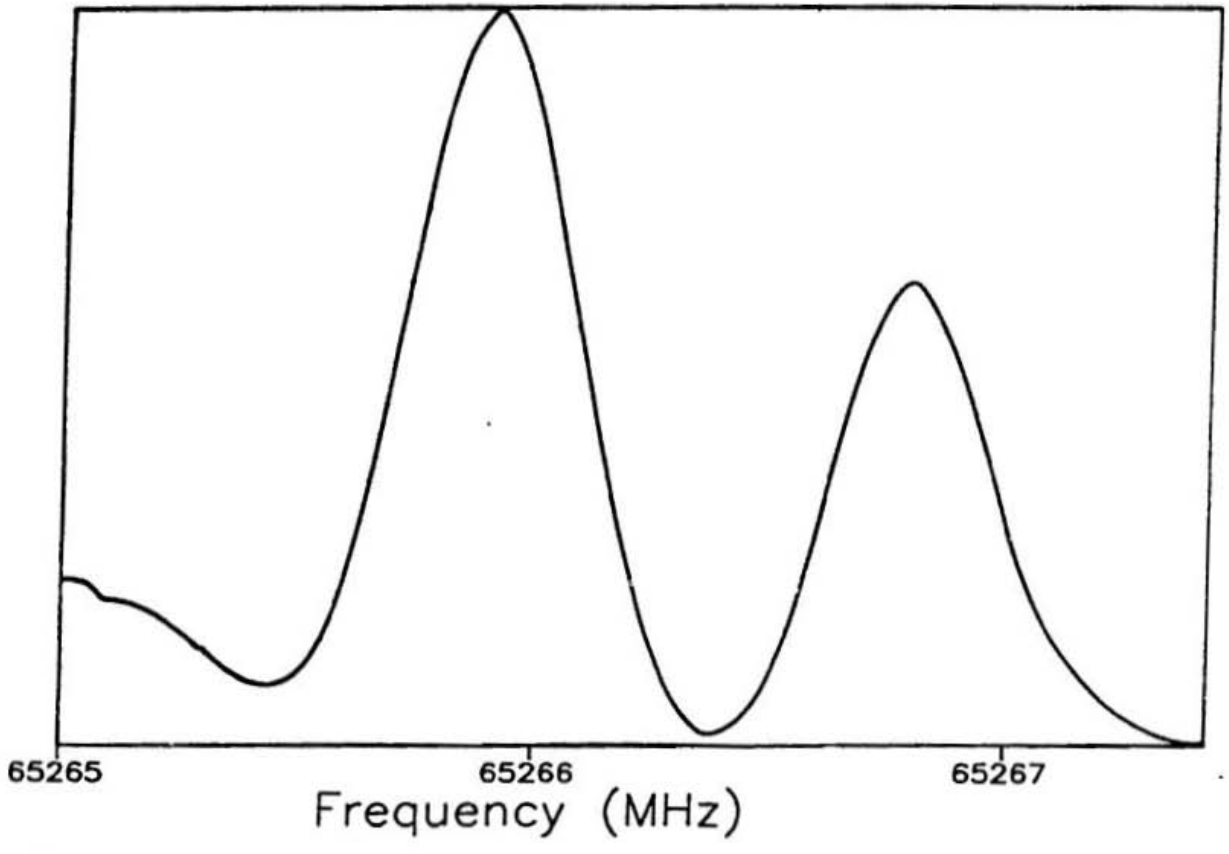

Figure 3.2: The $25_{2\,24} \leftarrow 24_{1\,24}$ and $25_{1\,24} \leftarrow 24_{0\,24}$ Rotational Transitions of 2-Chloropyrimidine

Table 3.19: Determinable Chlorine Quadrupole Coupling Constants in the Measured Isotopomers of 2-Chloropyrimidine[a]

	Normal Species	2-^{13}C	1,3-^{15}N	^{37}Cl	2-^{13}C,^{37}Cl	1,3-^{15}N,^{37}Cl
χ_{aa} / MHz	-71.78(16)	-72.0(20)	-72.09(23)	-56.4(8)	-56.(7)	-58.1(15)
η / MHz	-0.20(10)	-0.12	-0.18(13)	-0.7(4)	-0.19	-0.04

[a] Errors in brackets are in units of the last significant digit and represent uncertainties in the 95% confidence interval. Where no uncertainty figures are given, the magnitude of the error was the same as or larger than the value

3.2.1 Nitrogen Quadrupole Coupling Constants

All of the Q-branch transitions of 2-fluoropyrimidine showed a characteristic hyperfine splitting due to the presence of two equivalent quadrupolar nitrogen nuclei. In the high J limit, the selection rule $\Delta I = \Delta J$ holds roughly, and the hyperfine components coalesce into observable triplets [9]. Assignment of the components observed in rotational transitions was made by transferring the quadrupole coupling constant values measured for pyrimidine [10] (with the χ_{aa} and χ_{bb} values interchanged to reflect the differing inertial symmetry of these two molecules) and using standard formulas for quadrupolar energy levels in a molecule containing two equivalent couplings [11].

Deviations from the unperturbed rotational frequency within a given transition were used as data in the least squares. Since the observed hyperfine components were not symmetrically disposed about the unsplit line frequency, it was necessary first to obtain values of the

unperturbed rotational frequency from center of gravity calculations.

The formula for the unperturbed center frequency is given as

$$\nu_0 = \nu_2 - \frac{1}{3}(\nu_2 - \nu_1)$$

Splittings obtained for selected Q-branch rotational transitions in 2-fluoropyrimidine are given (Table 3.20). The principal element of the nitrogen quadrupole coupling tensor in the inertial frame, χ_{aa}, is determined from splittings in R-branch spectra. Hyperfine structure of this type was not resolved in the frequency region studied here; this demonstrates that χ_{aa} is very small for 2-fluoropyrimidine. From the observed splittings in the measured Q-branch transitions, the asymmetry in the quadrupole tensor $(\chi_{bb} - \chi_{cc})$ was well determined as 5.206(57) MHz.

In the high J limit the relative intensities of the hyperfine components are governed by their spin statistical weights. The rotation C_2^a of 2-fluoropyrimidine exchanges two equivalent fermions (hydrogen), and the total wave function must be antisymmetric with respect to this operation. With integral values of I_1 and I_2, the lowest 'pseudo' quantum state i is antisymmetric, with alternating parity as i increases. Thus the $i = 0, 2$ (6 functions) states are symmetric, while the $i = 1$ (two functions) states are antisymmetric with respect to this rotation. Spin weights are thus assigned to hyperfine components as 3 for components with $i = 0$ and 2, and 1 for components with $i = 1$ with $oo \leftrightarrow oe$ transitions and 1 for components with $i = 0, 2$, and 3 for components with $i = 1$ with $ee \leftrightarrow eo$ transitions. Examples of the hyperfine structure observed in the two different types of rotational transitions are illustrated in Figures 3.3 and 3.4.

Table 3.20: Some Examples of Hyperfine Splittings Observed for 2-Fluoropyrimidine

J_u	K_A	K_C	J_l	K_A	K_C	I'	I	F'	F	Obs	Obs-Calc
19	5	15	19	3	16						
						2	2	19	19	52671.490	-0.072
						0	0	19	19		-0.005
						1	1	19	19	52670.743	-0.006
						2	2	17	17		0.016
						2	2	21	21		-0.026
						2	2	18	18		0.036
						1	1	20	20	52671.159	-0.008
						1	1	18	18		0.013
						2	2	20	20		-0.027
19	4	15	19	4	16						
						0	0	19	19		0.026
						1	1	19	19	50876.663	0.024
						2	2	17	17		0.052
						2	2	21	21		-0.001
						2	2	18	18		0.030
						1	1	20	20	50877.151	-0.050
						1	1	18	18		-0.026
						2	2	20	20		0.001

References

[1] S. Cradock, P. B. Leischeski, D. W. H. Rankin, and H. E. Robertson, J. Am. Chem. Soc. 110, 2758 (1988).

[2] F. Michel, H. Nery, P. Nösberger, and G. Roussy, J. Mol. Struct. 30, 409 (1976).

[3] J. K. G. Watson in *Vibrational Spectra and Structure, a Series of Advances* (J. R. Durig, Ed.), Vol. VI, pp. 1-89, Elsevier, New York, 1977.

[4] H. D. Rudolph, Z. Naturforsch. 23a, 540 (1968).

[5] S. Nakama, H. Shimada, and R. Shimada, Bull. Chem. Soc. Japan, 57, 2584 (1984).

[6] C. C. Costain, J. Chem. Phys. 29, 864 (1958)

[7] W. Gordy and R. L. Cook, Microwave Molecular Spectra, John Wiley, New York, 1984.

[8] R. M. Sternheimer, Phys. Rev. A, 6 1702 (1972).

[9] V. Dobyns and L. Pierce, J. Am. Chem. Soc. 85, 3553 (1963).

[10] G. L. Blackman, R. D. Brown, and F. R. Burden, J. Mol. Spec. 35, 444 (1970).

[11] G. W. Robinson and C. D. Cornwell, J. Chem. Phys. 21, 1436 (1953).

4 Discussion

The results of the microwave investigation of the two species presented here may be discussed on two separate fronts. Changes in the structure of the pyrimidine ring give indication of perturbation of the hybridized molecular orbitals due to the presence of the substituted halogen. And quadrupole coupling constants observed for chlorine and nitrogen may be used to give some insight into the bonding in each molecule and may be directly compared with the results of electric field gradient calculations obtainable from *ab initio* and semi-empirical methods. We first consider the interpretation of the coupling constants obtained for 2-chloropyrimidine.

Table 4.1 shows the measured chlorine quadrupole coupling constants obtained in this investigation for 2-chloropyrimidine, along with those previously obtained for 2-chloropyridine, chloropyrazine, and chlorobenzene. There is a noticeable increase in the asymmetry of the tensor when comparing chlorobenzene, chloropyridine, and chloropyrimidine which indicates a growing imbalance in p orbital populations in the C–Cl bond and thus larger contributions from the ionic canonical forms of the molecule. The constants determined experimentally for 2-chloropyrimidine are given in the principal axes of the carbon chlorine bond, and thus may be directly compared with theoretical models. SCF calculations of the electric field gradient tensor around chlorine were performed for 2-chloropyrimidine and chlorobenzene at the 3-21G basis set level. With a value of the chlorine nuclear quadrupole moment, it was possible to obtain calculated values of the quadrupole coupling constants in each molecule (Table 4.2). Both calculations yielded good estimates of the principal element of the quadrupole tensor, but failed to reproduce the sign of the asymmetry parameter η; it is encouraging to

note, however, that the asymmetry is predicted to increase from chlorobenzene to chloropyrimidine.

Some understanding of the variation in bond character between the presented chlorinated aza aromatics may also be had by considering changes in the C-Cl bond length. It has been previously stated that there is a direct correlation between this quantity and the degree of asymmetry in the quadrupole tensor [4]. In the comparison given here, previously obtained structural data may not warrant close examination, as only a 'partial' ground state geometry has been obtained for 2-chloropyridine [8], and some doubt must be placed on the small uncertainty in the carbon chlorine substitution bond length reported for chlorobenzene [5]. Additionally, steric repulsion due to the presence of the two adjacent nitrogen lone pairs may offset any contraction in the carbon chlorine bond length in 2-chloropyrimidine due to hyperconjugation and thus may limit the validity of this comparison. It is interesting to note, however, that in addition to correctly predicting the trend in electric field gradient asymmetry for chlorobenzene and chloropyrimidine, the low level *ab initio* calculations also predict a decrease in carbon chlorine bond length, which is consistent with the existing experimental evidence.

In Table 4.3 the nitrogen nuclear quadrupole coupling constants of 2-fluoropyrimidine are compared with a number of related heterocyclic molecules. To facilitate comparison, the literature principal inertial axes quadrupole coupling constant values have been transformed so that the one axis in the plane lies parallel to the C—F bond. Nitrogen coupling constants obtained for both analogous pairs (pyrimidine and pyridine) are remarkably similar and show almost quantitatively the same change in the parameter $\chi_{bb} - \chi_{cc}$ with fluorine substitution. *Ab initio* calculations yielded predictions of the electric field gradients at nitrogen for pyrim-

idine and 2-fluoropyrimidine. From the recommended value of the quadrupole moment of nitrogen [3], it was possible to calculate quadrupole coupling constants pyrimidine and 2-fluoropyrimidine at the 3-21G basis set level (Table 4.2). These calculations perform poorly in light of the results obtained for chlorobenzene and chloropyrimidine, however the trend in asymmetry of the tensor ($\chi_{bb} - \chi_{cc}$) is reproduced. The large disagreement between the observed and calculated coupling constants is somewhat disconcerting, however this failing may have arisen primarily from the fact that the *ab initio* geometry may be in error, causing the transformation from the principal axes of the coupling to the inertial axes to be improperly defined. An accurate spectroscopic geometry will allow for axis transformation to that oriented along the bisector of the C-N-C bond angle, in order that a more judicious comparison with the *ab initio* result, which may be arbitrarily cast in any orientation, be made.

Geometrical distortions in the pyrimidine ring due to substitution at the 2 position are not entirely evident from the existing experimental data. This anomaly is compounded by the fact that there is no obvious trend in geometrical variation obtained from the *ab initio* calculations performed for the molecules. Additionally, it must be kept in mind that the present best gas phase geometry for pyrimidine is based mainly on the results of electron diffraction [13] and thus represents a thermally averaged rather than a state specific structure. Pyrimidine is an excellent candidate for a substitution geometry, as none of the nuclear coordinates lie close to the inertial axes. Searching for naturally occurring isotopomers is difficult, however, owing to the dominance of Q branch transitions from the normal species in the spectrum. An improved guess of the molecular geometry should help narrow the search range for the naturally occurring isotopomers; alternatively, it should be possible to

synthesize enriched samples of the compound, as was done for 2-chloropyrimidine.

References

[1] S. Akavipat, C. F. Su, R. L. Cook, J. Mol. Spec. 111, 209 (1985).

[2] M. Meyer, U. Andersen, and H. Dreizler, Z. Naturforsch. 42a, 197 (1987).

[3] W. Caminati and A. M. Mirri, Chem. Phys. Lett. 12, 127 (1971).

[4] E. A. C. Lucken, Nuclear Quadrupole Coupling Constants, Academic Press, New York (1969).

[5] F. Michel, H. Nery, P. Nösberger, and G. Roussy, J. Mol. Struct. 30, 409 (1976).

[6] G. L. Blackman, R. D. Brown, and F. R. Burden, J. Mol. Spec. 35, 444 (1970).

[7] G. O. Sorensen, J. Mol. Spec. 22, 325 (1967).

[8] S. D. Sharma, S. Doraiswamy, H. Legell, H. Mäder, and D. H. Sutter, Z. Naturforsch. 26a, 1342 (1971).

[9] O. L. Stiefvater, S. Liu, and J. A. Ladd, Z. Naturforsch. 31a, 53-60 (1976).

[10] G. E. Scuseria, T. J. Lee, R. J. Saykally, and H. F. Schaefer, J. Chem. Phys. 84, 3711 (1986).

[11] S. Cradock, P. B. Leischeski, D. W. H. Rankin, and H. E. Robertson, J. Am. Chem. Soc. 110, 2758 (1988).

Table 4.1: Chlorine Quadrupole Coupling Constants of 2-Chloropyrimidine and Related Molecules

	2-chloropyrimidine[a]	chloropyrazine[b]	2-chloropyridine[c]	chlorobenzene[d]
χ_{aa}/MHz	-71.98(16)	-71.64(13)	-70.42(4)	-71.09(10)
χ_{bb}/MHz			39.69(2)	38.18(49)
χ_{cc}/MHz			30.73(4)	32.91(50)
η	-0.20(10)	-0.13	-0.1272	-0.0741

[a] this work

[b] reference [6]

[c] reference [8]

[d] reference [7]

Table 4.2: SCF Values of Chlorine and Nitrogen Quadrupole Coupling Constants [a]

	2-Chloropyrimidine	Chlorobenzene	2-Fluoropyrimidine	Pyrimidine
χ_{aa}	-73.04	-70.53	-2.93	-3.475
χ_{bb}	32.32	40.72	-2.06	-1.67
χ_{cc}	40.72	35.56	5.146	4.83

[a] values obtained with the 3-21G basis set at the restricted Hartree Fock level

Table 4.3: Quadrupole Coupling Constants in 2-Fluoropyrimidine and Related Molecules

	$\chi_{\parallel}$ / MHz	$\chi_{\perp}$ / MHz	χ_{cc} / MHz
2-Fluoropyrimidine [a]	0.0	-2.60	2.60
Pyrimidine [b]	-0.223	-3.107	3.330(14)
Pyridine [c]	-0.15	-3.30	3.45(2)
2-Fluoropyridine [d]	-0.02	-2.80	2.82(5)
2,6-Difluoropyridine [e]	0.33	-2.67	2.34

[a] this work, $\chi_{\parallel}$ was assumed to be zero

[b] reference [9]

[c] reference [10]

[d] reference [11]

[e] reference [12]